CONTROLLED HIGH PRESSURE SLURRY INJECTION IN WATER JETTING APPLICATIONS-A NEW APPROACH

A Thesis

Submitted to the Graduate Faculty of the
Louisiana State University and
Agricultural and Mechanical College
in partial fulfillment of the
requirements for the degree of
Master of Science in Petroleum Engineering

in

The Department of Petroleum Engineering

by
Manish Kumar
B.S., Maharshi Dayanand University, India, 2002
December 2005

To Alka
“Could not have made it this far without her”

ACKNOWLEDEGEMENTS

The author wishes to express his sincere gratitude to Dr. Anuj Gupta, Associate Professor of Petroleum Engineering Department at Louisiana State University, under whose guidance and supervision this work was conducted.

For their much appreciated help and suggestions, a special thanks is extended to Dr. Julius Langlinais, as well as to Mr. Gerry Masterman whose valuable assistance was required during the experimental phase of the project and to Dr. D.N. Rao to serve on the committee.

The author also recognizes CAD Control Systems for providing pressure accumulators used during the study, which was provided at no cost to Louisiana State University and Kelco Oilfield Group for generously providing essential Polymers used in experiments.

The author also appreciates Patrick Slattery and Kanishk Rastogi for their invaluable help in conducting experiments.

TABLE OF CONTENTS

LIST OF TABLES

LIST OF FIGURES

ABSTRACT

The ability of an abrasive assisted water jet to cut through rocks and metals has potential applications in the oilfield. However, the size of cutting nozzle has not allowed water jet to be used on commercial scale for drilling reservoir rocks down-hole. Inefficient momentum transfer to abrasive particles from pressurized water and lack of abrasive feed rate control in commercially available units has further discouraged the use of water jet in oil industry.

Despite various technical difficulties, immense power of water jet cannot be neglected. Studies have shown that momentum transfer can be improved significantly, if abrasive particles are introduced upstream of the nozzle. Limited techniques are available where abrasives are first suspended in a fluid stream and are then introduced in high-pressure water stream upstream of the nozzle. However, control over abrasive feed rate was lacking in past studies.

In this investigation, an experimental apparatus was assembled a polymer solution was injected upstream of the nozzle. Injection rate was controlled, by varying the rpm of the plunger pump. The apparatus was used to study the effect of Xanthan and Polyacrylamide on water jet coherency.

It is shown that addition of polymer leads to a focused water jet for a longer distance before it starts disintegrating into a mist. Furthermore, there is an optimum concentration of polymer at which the jet stays focused for the longest distance.

CHAPTER 1: INTRODUCTION

The concept of water jet was first introduced in 1960's and the initial applications were limited to cleaning and unblocking drains. It was not because researchers could not see the power of water jet, but because of the pressure limitation of then existing pumps and accessories. With the development of new technology and availability of high pressure pumps water jetting gained importance and was used on commercial scale to cut soft materials such as cardboard and rubber. Cutting of hard materials such as rock and steel was attempted, but did not succeed because it took enormous pressure levels to reach the threshold point where water jet could actually penetrate and erode the target surface. The solution to this problem appeared to be the introduction of abrasive material in high-pressure water stream.

Many different abrasive injection methods were developed and some of them worked very well. However, controlled and efficient abrasive injection continues to be an unresolved problem. Many efforts were made in late 1960's to use water jetting in petroleum industry to drill sub-surface reservoir rocks, but favorable results could not be achieved because of deficient abrasive injection techniques [1], [2], [3], [4]. When abrasives were pumped along with water using a positive displacement pump, the process became uneconomical because of prompt wear of pump liners and valves by abrasives. Current commercially available units are not suitable for use in petroleum industry especially when the goal is to efficiently cut sub-surface rock using water jet. Bulkier cutting head and large pressure drop requirement upstream of the cutting nozzle make currently available units ineffective for down-hole operations.

A detailed discussion of problems associated with currently available abrasive injection system are discussed in Chapter 2, but basic principle, types, applications and advantages of water jet over mechanical methods will be introduced in the following sections.

1.1 Principle of Water Jet

Water jet is generated by pressurizing water to high-pressure levels (1,000 psi – 20,000 psi) using a high-pressure water blaster, which is basically a triplex pump, and then accelerating it through a small nozzle opening. Figure 1 depicts general flow diagram of water jetting component [5].

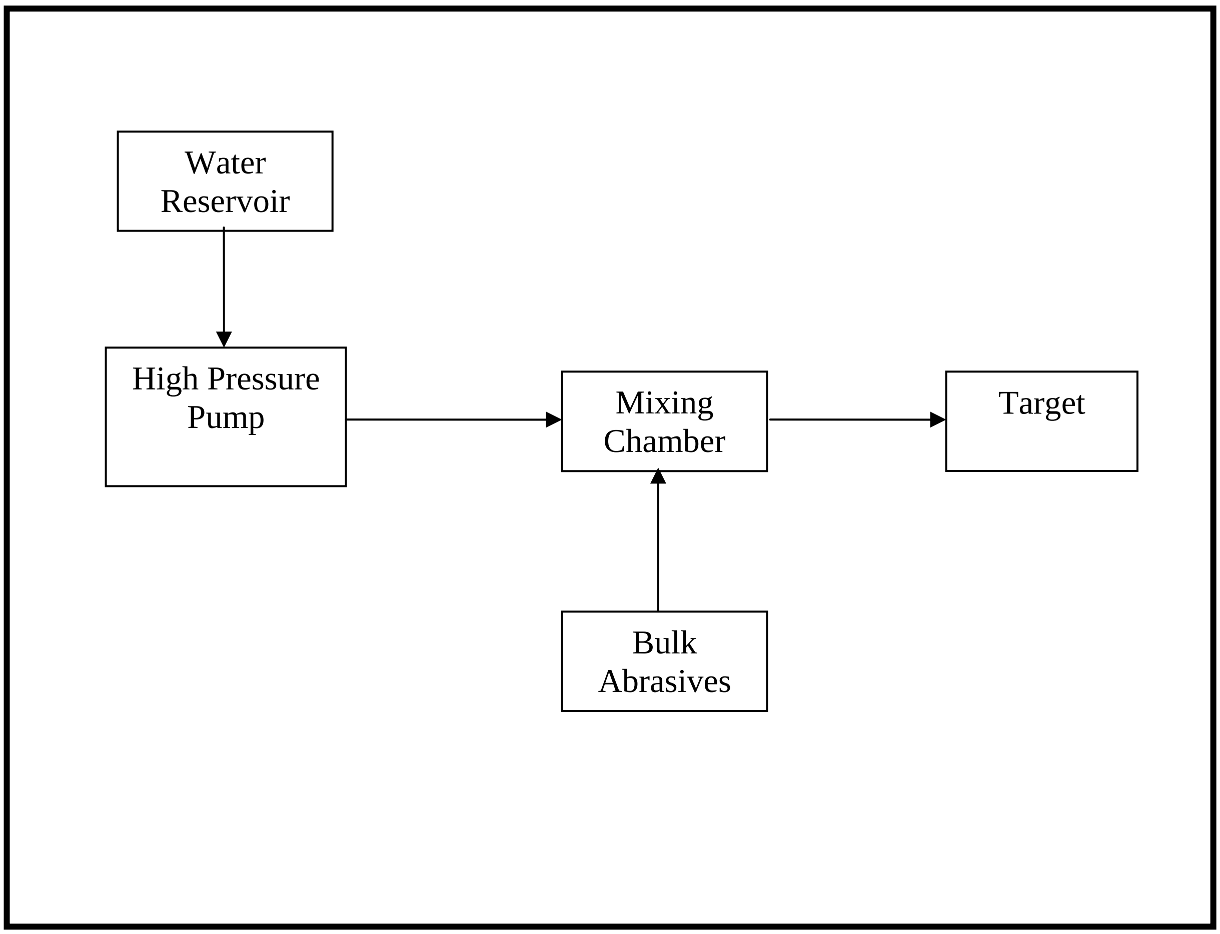

Figure 1 Water Jetting Components

Nozzle is made of brass or steel and is sometimes lined with an insert of tungsten carbide to withstand the abrasion from abrasive particles in the pressurized water stream accelerating past the nozzle. Stainless steel nozzle without an insert can be used if abrasives are not in use. Cutting by water jet is believed to occur due to micro level abrasion and erosion of the target surface by abrasive particles. It is also believed and has been experimentally proven that sharp edged abrasive particles tend to provide better cutting results [5], [6], [7].

1.2 Advantages of Water Jetting

Water jet is routinely used on commercial scale for industrial cleaning and machining. With easier availability of pressure boosters water jetting has gained acceptance for yard cleaning and other domestic applications. Heat generation has always been a problem with mechanical or laser machining and cutting; whereas no heat is generated with water jet based cutting and work piece is not exposed to detrimental thermal stresses.

1.3 Types of Water Jet

Water jet is categorized as plain if only water is used for jetting and abrasive assisted if abrasives are introduced in high-pressure water stream to accomplish a certain task.

Table 1 Types of Water Jet

Plain Water Jet	**Abrasive Assisted Water Jet**	
Soft Rubber	Titanium	Aluminum
Thin Foil	Stone	Copper
Cardboard	Granite	Stainless Steel
Foam	Ceramics	Marble
Soft Gasket	Glass	Plastics

For most applications garnet sand is the preferred abrasive because of the ease of availability, and hardness comparable to that of diamond. Currently, plain water jet is used for mild cleaning. For all other applications, starting from paint removal to machining, abrasive assisted water jet is preferred. Table 1 details some of the tasks that can be accomplished using water jet. However, efforts are under progress to utilize the immense power of abrasive assisted water jetting technology in fields like petroleum engineering where it could be used to drill slim lateral holes and could contribute to blowout control by assisting cutting of burning well heads and by providing a safer working distance to fire fighting crew.

1.4 Abrasive Assisted Water Jet

The cutting ability of water jet can be dramatically improved by introducing hard particles, usually know as abrasives into the high velocity water stream. Garnet sand is commonly used as an abrasive on commercial scale for cleaning and cutting purposes. Unfortunately, abrasive particle causes severe wear problems to the parts downstream of the abrasive injection point, especially the cutting nozzle and the collimator tube. Efforts are underway to design an efficient system to utilize abrasive cutting power with minimum wear problem. Chapter 2 describes various schemes for injecting abrasive particles in high velocity water stream in more detail.

1.5 Factors Governing Water Jet Cutting Performance

The cutting performance of a water jet depends on many parameters. Such factors have been examined in great details by various researchers over last four decades. This section summarizes the effect of parameters relevant to this study.

1. Water Jet Pressure: Water jet pressure and depth of cut follow a linear relation after the critical pressure is reached as shown in Figure 2 [8]. Critical pressure depends on a material's erosion characteristics and would be independent of abrasives and mixing parameters if the material could be cut with plain water jet [9], [10].
2. Abrasive Particle Size: There is no clear definition of abrasive particle size that would generate deepest cuts for a given material. In general, the depth of cut improves with

increase in particle size, but the largest particle size is limited by the nozzle opening. Normally, it is recommended to use the abrasive particle size smaller than one third of the nozzle diameter. [9], [10], [11], [12].

3. Abrasive Flow Rate: Abrasive flow rate plays a critical role in abrasive-assisted water jet performance.

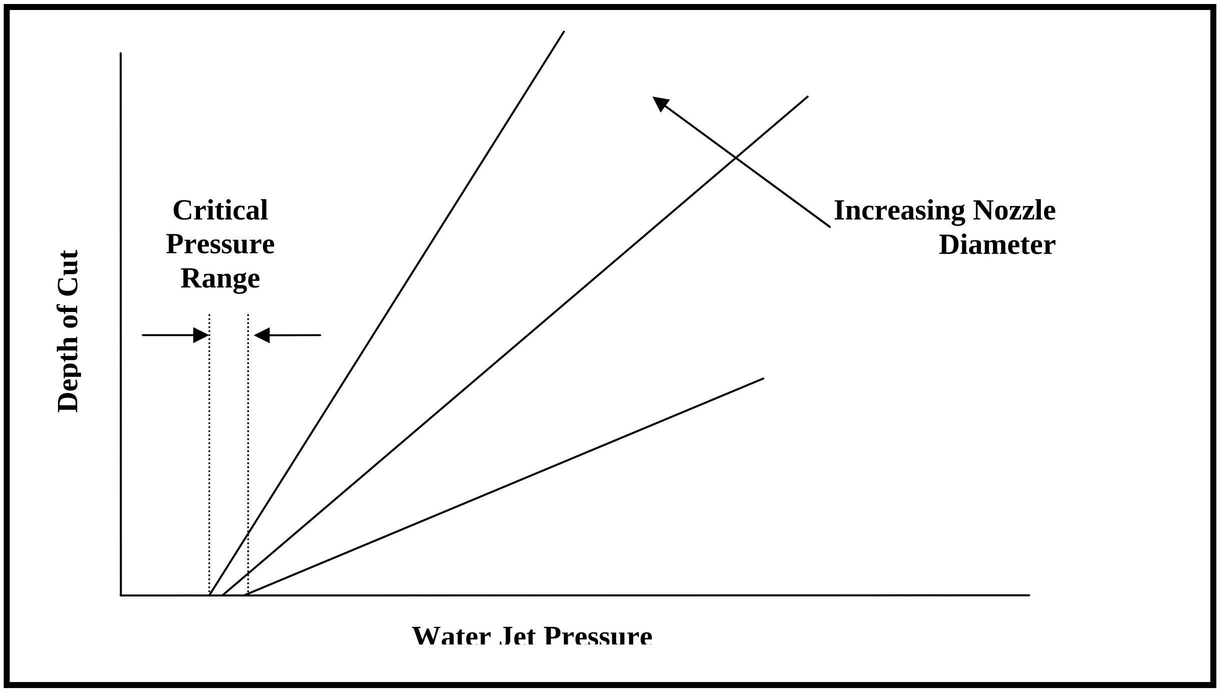

Figure 2 Effect of Pressure on Depth of Cut [9]

Detailed discussion of its effects on cutting performance, various problems associated with commercially available abrasive injection unit and the need to gain a control on abrasive feed rate is incorporated in Chapter 2.

CHAPTER 2: LITERATURE REVIEW

2.1 Introduction

Many studies have been conducted to understand the effect of the amount of abrasives entrained in the high velocity water stream on cutting performance of abrasive water jet and it has been established that initially the abrasive flow rate and depth of cut follows a linear relationship [8]. However, beyond the optimum point any further increase in abrasive flow rate leads to a decrease in the depth of cut [8]. Based on theory of erosion, the depth of cut is proportional to a particle's kinetic energy and depends on the particle velocity exiting the nozzle [9]. Depth of Cut (h) α Kinetic Energy

$$h \propto Mv^2 \quad \text{-----------------------------------} (2.1)$$

Where, M is the mass of a particle and v is its exit velocity.

In terms of water jet velocity (v_j) [9],

$$v \approx v_j \frac{1}{1+R} \quad \text{----------------------------------} (2.2)$$

Where, R is the loading ratio and can be described as the ratio of abrasive flow rate (m) over water flow rate (m_w).

$$R = \frac{m}{m_w} \quad \text{-------------------------------------} (2.3)$$

Using equation (2.2) in (2.1), the depth of cut can be estimated based on erosion theory as:

$$h = M\left(\frac{v_j}{1+R}\right)^2 \quad \text{--------------------------------} (2.3)$$

Where, the critical abrasive flow rate is obtained at $\frac{\partial h}{\partial R} = 0$.

However, there is a discrepancy in the valves of critical flow rate obtained from Equation 2.3 and from experiments, which is usually attributed to mixing losses at the point of injection [9]. A plot between depth of cut and abrasive flow rate would generally yield results as shown in Figure 3.

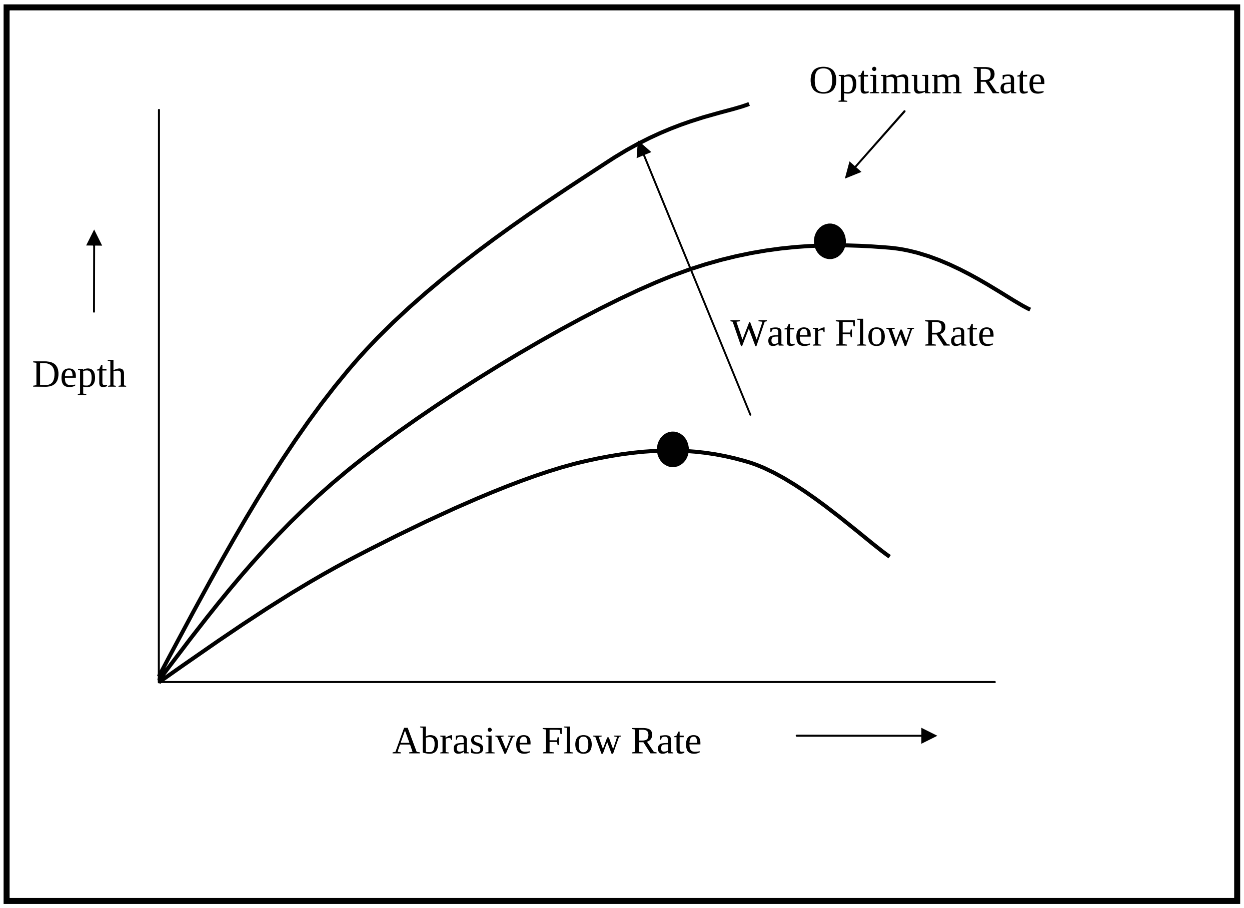

Figure 3 Optimum Abrasive Feed Rates [9]

Above discussion signifies the importance of controlled abrasive feed rate. If, abrasive flow rate is less than optimum amount, sufficient cut may not be achieved and on the contrary if it were too high, abrasives would be wasted. Since the beginning of abrasive assisted water jetting, various techniques have been employed to gain effective and efficient control over abrasive feed rates. Following sections would describe the governing principle, achievements and limitations of these techniques.

2.2 Abrasive Injection Techniques

Once it was established that abrasive water jet outperforms conventional water jet in terms of cutting performance and pressure requirement, abrasive injection became one of the critical issue along with problems related to erosion caused by abrasives on water jetting equipment. Starting from simple sand guns to pressurized hoppers and to the latest DIAjet solution also known as ASJ (Abrasive Slurry Jet), abrasive injection has continuously attracted researchers and engineers to develop an efficient abrasive injection system that could feed abrasive continuously in high pressure water stream without causing unnecessary pressure drop and provide control over the amount of abrasives entering the high pressure water stream.

Following sections of this Chapter concentrate on the abrasive injection techniques that are currently available and shed some light on the use of polymer to suspend abrasive particles and boost water jet performance.

2.2.1 Post-Orifice Injection

Post-Orifice Injection is a process of mixing abrasives with pressurized water downstream of the pump. This avoids pump wear and provides better results in terms of cutting and cleaning. As pressurized water is forced to pass through a small opening or an orifice the resulting pressure drop creates suction in a mixing chamber that allows abrasive entrainment. The amount of suction and abrasive entrainment is proportional to the pressure drop. The mixing of abrasive and water takes place in a mixing chamber and the slurry is transferred to a focusing nozzle by a collimating or discharge tube. A typical abrasive feed system, shown in Figure 4, consists of a bulk abrasive storage, usually a hopper, an attached tubing that transports abrasive to the injection point where abrasives are introduced in the high pressure water stream and are accelerated by high velocity water to create an erosive impact on the target surface. This technique has been in use for last two decades and is used for surface applications such as machining, cleaning and cutting. Some of the major limitations of Post-Orifice Injection techniques are discussed below.

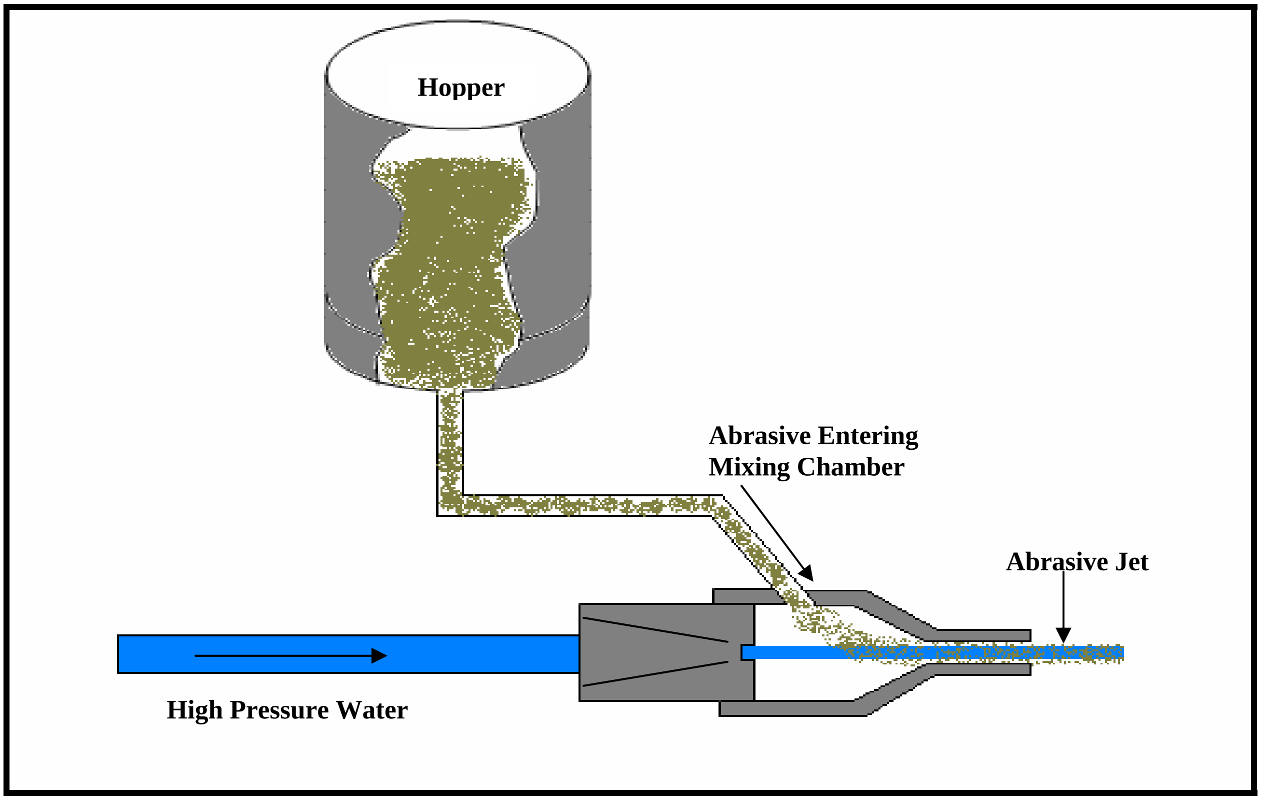

Figure 4 Hopper and Cutting Head used in Post-Orifice Abrasive Injection

1. Nozzle faces severe and rapid erosion from abrasive slurry. To reduce the severity of erosion almost all water jetting focusing nozzles have a tungsten carbide insert.
2. There is a misconception that the Post-Orifice Injection doesn't require any external source of energy to mix abrasives and water. However, the pressure drop occurring at the nozzle provides the required energy. This limits the useful pressure drop that would have been available at the focusing nozzle, and, as a result, reduces the jet impact force which is directly proportional to the pressure drop across the focusing nozzle.
3. Another major problem with dry abrasive feed system using an eductor assembly is the lack of control over abrasive feed rate. Abrasive feed rate in an eductor is governed by

suction pressure in the mixing chamber, which depends on the orifice size. So it is nearly impossible to control the abrasive feed rate with a single orifice in order to attain an optimal abrasive feed rate. The possible, but impractical, alternate is to keep on changing the orifice size until an optimal abrasive feed rate is achieved. Further, the abrasive feed rate changes as the orifice opening changes due to erosion.

4. Air entrainment is another critical problem with post orifice injection, especially when Post-Orifice assembly is used for dry abrasive feed. As air gets into the system it causes two main problems: (a) three phase flow in the collimator tube, and, (b) when air leaves the jet it expands and breaks the jet in droplets, significantly reducing the cutting performance [13], [14].
5. Liquid build up in abrasive feed line is another issue. This happens when water from mixing chamber gets inside the abrasive feed line. Water mixes with abrasive and causes clogging problems.

2.2.2 Pressurized Hopper

Pressurized hopper prevents liquid build up in abrasive feed line by applying air pressure on top of the dry abrasives inside the hopper. Abrasives are stored in a hopper, which is pressurized using compressed air. A slipstream of compressed air carries the abrasives from the bottom of the hopper to the mixing chamber. Pressurized hopper takes care of liquid hold up problem by not allowing water from mixing chamber to enter back in the abrasive feed line, but adds to the problem of air entrainment. Air entrainment causes critical impact on the performance of water jet by expanding the jet as it leaves the cutting nozzle. As an air bubble expands it disintegrates the jet and causes poor precision.

2.2.3 DIAjet (ASJ) Solution

To avoid air entrainment in the mixing chamber DIAjet (Direct Injection of Abrasive JETting) introduced a method of abrasive injection by injecting abrasives directly upstream of the cutting head and was first introduced in a Master's Thesis by Cranfield [16]. Schematic of DIAjet technique is shown in Figure 5.

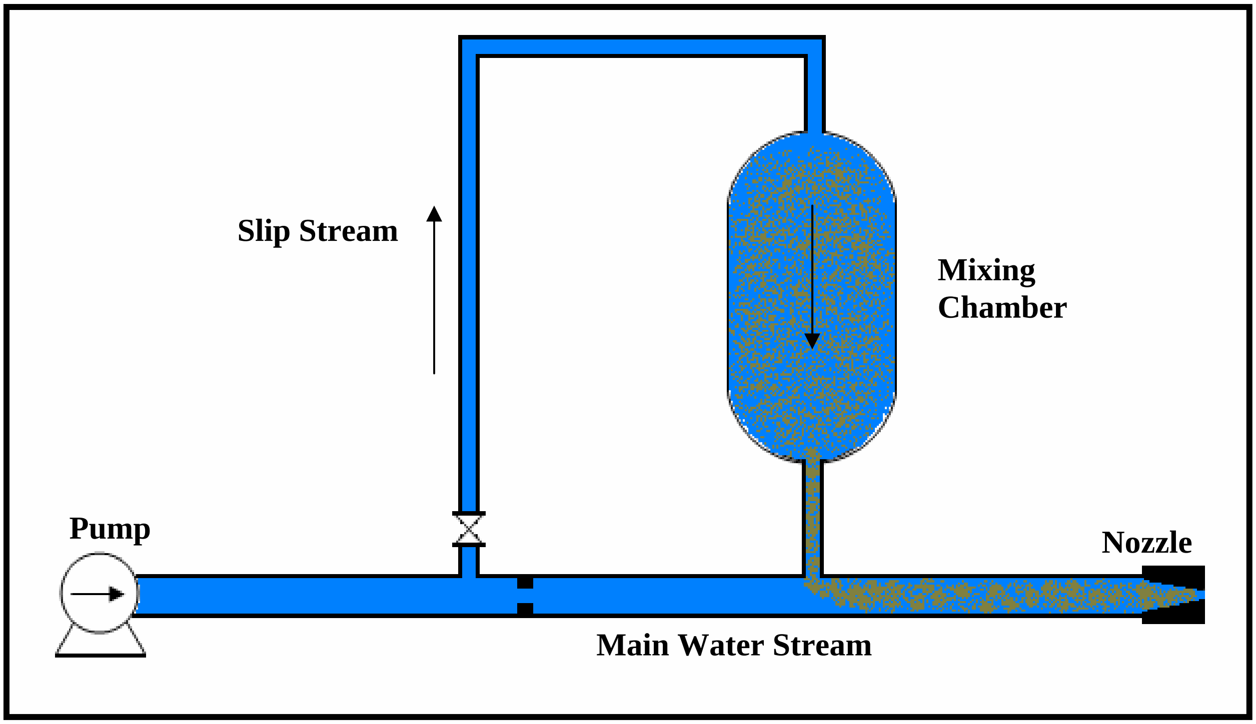

Figure 5 Schematic of DIAjet Technique [15]

DIAjet utilizes a slipstream of the motive fluid to inject abrasives. Usually 10% of the motive fluid is directed to a vessel where it mixes with the abrasive particles. The mixture of water and abrasive is delivered to the cutting head without any air entrainment. In order to ensure that pressure of the main stream at the injection point is less the pressure of the slurry in the vessel, a small restriction is usually placed downstream of the slipstream. This design eliminates air entrainment as no air is introduced in the system, but the problem of controlling abrasive feed rate still exists as there is no way to ensure that the slip stream would deliver same concentration of abrasives throughout the injection cycle.

2.2.4 Bladder Transfer System

The approach to abrasive injection discussed above is indeed a dilution process, as there is no barrier between the abrasives being injected and water entering the vessel as slipstream. So, with time, the amount of abrasives being injected decreases, because the water flow rate to the vessel is constant, but abrasive contents with-in the vessel decrease continuously.

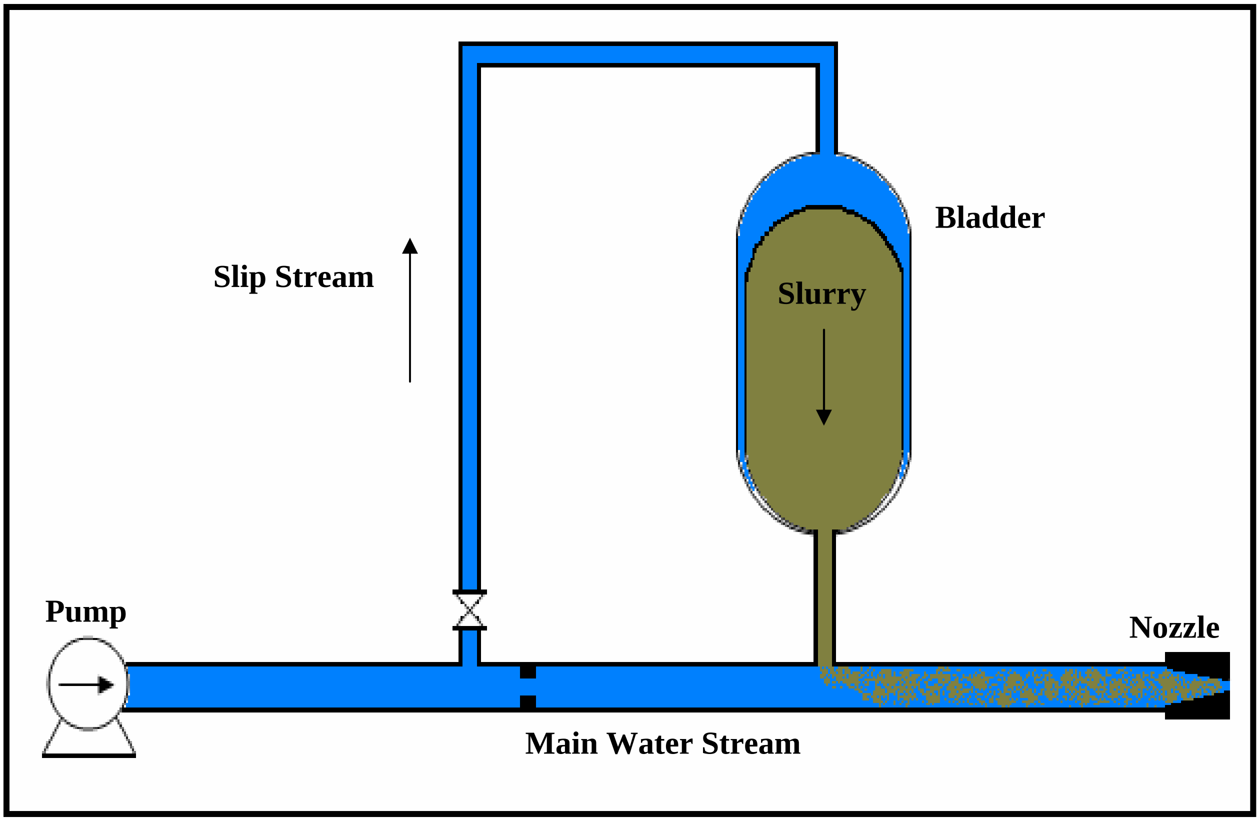

Figure 6 Schematic of Bladder Transfer System [16]

Decreasing abrasive concentration results in a reduction of the cutting ability of the jet. In order to maintain a constant abrasive feed rate, it is imperative to have barrier, separating water from abrasives. Chacko etal developed a method based on this concept at The University of Missouri-Rolla [16]. General process schematic was similar to that used by DIAjet, except an improvement in the pressure vessel containing the abrasives. The modification included a rubber bladder to prevent mixing of water and abrasives. Moreover, the abrasive particles were suspended in polymer slurry, which made abrasives easier to inject. Schematic of this technique is shown in Figure 6. Similar apparatus was developed at The University of Alabama, Tuscaloosa. Their apparatus however, consisted of two accumulators and was used for drilling small holes in reinforced concrete [17].

Polymer fulfills the critical role of suspending abrasives in water. In order to achieve a constant abrasive feed rate it is important that the polymer provide a stable suspension of abrasive particles. If suspension is not stable, abrasive particles tend to settle down under gravity causing a higher abrasive concentration at the bottom of the bladder.

Limitations of bladder transfer system, as developed at the University of Missouri-Rolla, are discussed below:

1. The pressure of water in the main fluid stream at the point of abrasive injection must be lower than the slipstream pressure that compresses the bladder. This can be achieved by placing a restriction downstream of the slipstream, but would limit the pressure drop at the cutting nozzle.
2. Abrasive loading cannot be increased without changing the slipstream flow rate, which would cause a fluctuation in motive fluid stream.
3. In practical terms, the flow split between the primary and the slipstream depends on the pressure losses in each path. As the slurry transfer from the bladder progresses, the frictional losses change thus changing the abrasive feed rate.

2.2.5 Piston Transfer System

A piston assembly as shown in Figure 7 is based on the same principle as the bladder discussed in the preceding. The only difference is that it uses a piston to separate the abrasives slurry added to the high-pressure water stream. This design was tested at Rock Mechanics and

Explosive and Research Centre at The University of Missouri-Rolla, Missouri. The piston assembly included a polished cylinder and a floating metallic disc or a piston head without rod. Metal to metal seal between polished cylinder and piston avoids abrasive dilution. O-ring seal is not recommended in an abrasive environment, as abrasive particle would wear it very rapidly.

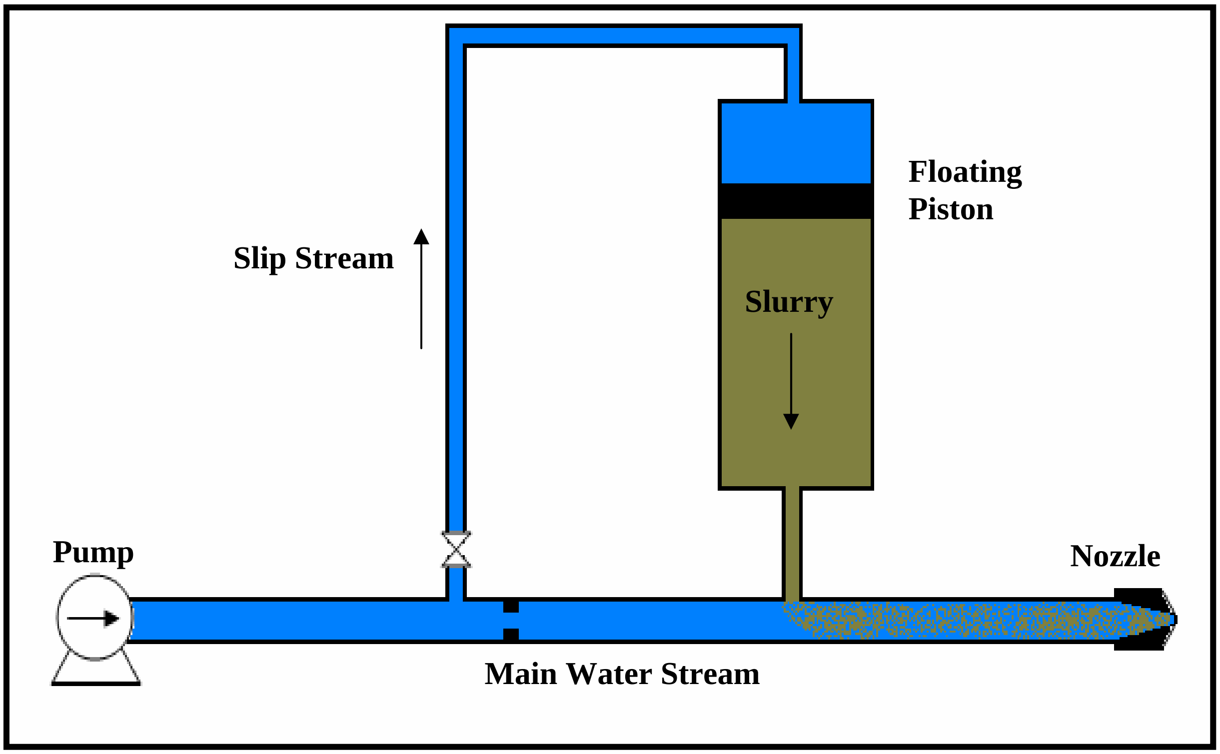

Figure 7 Schematic of Piston Transfer System

Slipstream from high-pressure water pump provides pressure on top of the piston to force the abrasive slurry in the high-pressure water stream. Abrasive particles are suspended in a polymer to make slurry before feeding to the assembly as it facilitates piston to slide. The limitations associated with piston assembly are:

1. It requires excess pressure to push the piston vertically downward because of friction between the piston and the cylinder wall.
2. Piston may get stuck when abrasive particles get in between the piston and the cylinder wall.

3. Abrasive particles also lead to excessive wear of piston and cylindrical walls.
4. Generates considerable heat due to friction caused by sliding piston.

2.3 Polymer Blasting

In 1883 increased flow rates were recorded in a silt laden river [18], but this phenomenon couldn't be explained until 1963 when Savins [19] coined the term "Drag Reduction" caused by certain additives in water. An article published in New Scientist, in 1964, reported that when SodiumCarboxyMethylCellulose (CMC) left the fire fighting hose nozzle, the water didn't disperse into the wind for a longer distance [20]. However, pertaining to this discussion, Summers [21] described the use of polymer as valuable additive in high pressure water blasting. Later in 1973, Russian workers found that metallic obstacles could be destructed more efficiently using a dilute solution of polymer. Same effects were recorded at Chevron U.S.A, Richmond Refinery, in California when SUPER-WATER® was used to clean heat exchangers [22]. For abrasive water jet cutting, addition of polymer could substantially improve water jet cutting ability [22]. In addition, the presence of polymer in water could significantly reduce frictional pressure losses [23], [24].

2.3.1 Polymers for Water Jet Cohesion

Different long chain polymers used in industry includes Polyacrylamide, Xanthan, Guar, etc. Guar is mostly used in Petroleum industry in hydraulic fracturing applications. Polyacrylamide is most widely used long chain synthetic polymer to improve water jet performance, but offers limited ability to hold abrasives in suspension. Further, the spills of polyacrylamide slurry are very slippery lead to safety hazard [16]. Xanthan has gained importance in terms of abrasive suspension. However, its ability to improve water jet performance has not been studied in detail.

2.3.2 Properties of Xanthan

Xanthan gum is widely used to improve the viscosity of a solution and provides stable suspensions. Xanthan is a common additive in drilling fluids and is used to improve the viscosity of the viscosity for better cutting suspension and thus, improving well-bore cleaning. Chemical structure of Xanthan is shown in Figure 8 and key properties of Xanthan are discussed below [25]:

1. High viscosity at low concentrations.
2. Unaffected by salinity (pH 2-12).
3. Salt tolerant viscosity builder.
4. Excellent temperature stability up to 300^{o}F.
5. Rapid hydration without lumping.
6. Reliable viscosity control.

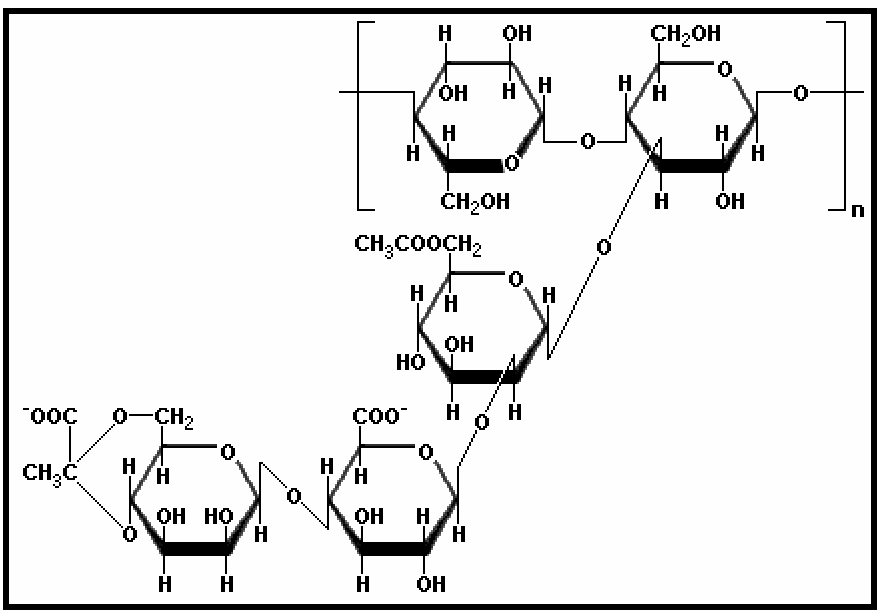

Figure 8 Structure of Xanthan (Source: www.scientificpsychic.com)

CHAPTER 3: ALTERNATE DESIGNS FOR ABRASIVE POLYMER SLURRY SYSTEM

3.1 Introduction

Considering the limitations of existing abrasive injection systems and the dependence of water jet quality on abrasive feed rate, there is a need to design and develop a system that would provide improved water jetting results, and would overcome the limitations of the existing injection systems, in terms of cleaning and cutting efficiency. The objectives of improved slurry injection techniques are summarized below:

1. To achieve the flexibility to adjust abrasive flow rate depending on application.
2. To maintain constant slurry concentration without dilution.
3. To achieve the largest available pressure drop at the cutting nozzle.
4. To eliminate any air entrainment at the point of abrasive injection.

Further, currently available commercially units are good for surface applications. If this system is to be used to perform any drilling or completion operation down-hole, the size of the cutting head must be reduced considerably. This can be achieved if the abrasive slurry is injected on the surface via high-pressure tubing. Commercially available Post-Orifice Injection technique can not be used in this case as it requires collimator tube diameter to be lager than orifice diameter in order to create negative pressure in mixing chamber.

Surface abrasive injection can be achieved if the abrasive slurry is forced into the main high-pressure water stream using an independent system that is capable of delivering slurry at enough pressure to over come the pressure of the main stream. This concept appears similar to DIAjet, Bladder and Piston assemblies already discussed in Chapter 2, but none of them were able to achieve control over abrasive feed rate. The proposed system is expected to achieve control over abrasive feed rate by controlling the delivery rate of the slurry system. This chapter concentrates on relative merits and feasibility of two designs utilizing an external source to deliver abrasives at controlled rates.

3.2 Design I

Design I utilizes a reversible motor to provide a linear displacement to a threaded shaft attached to it by means of gear arrangement, as shown in Figure 9.

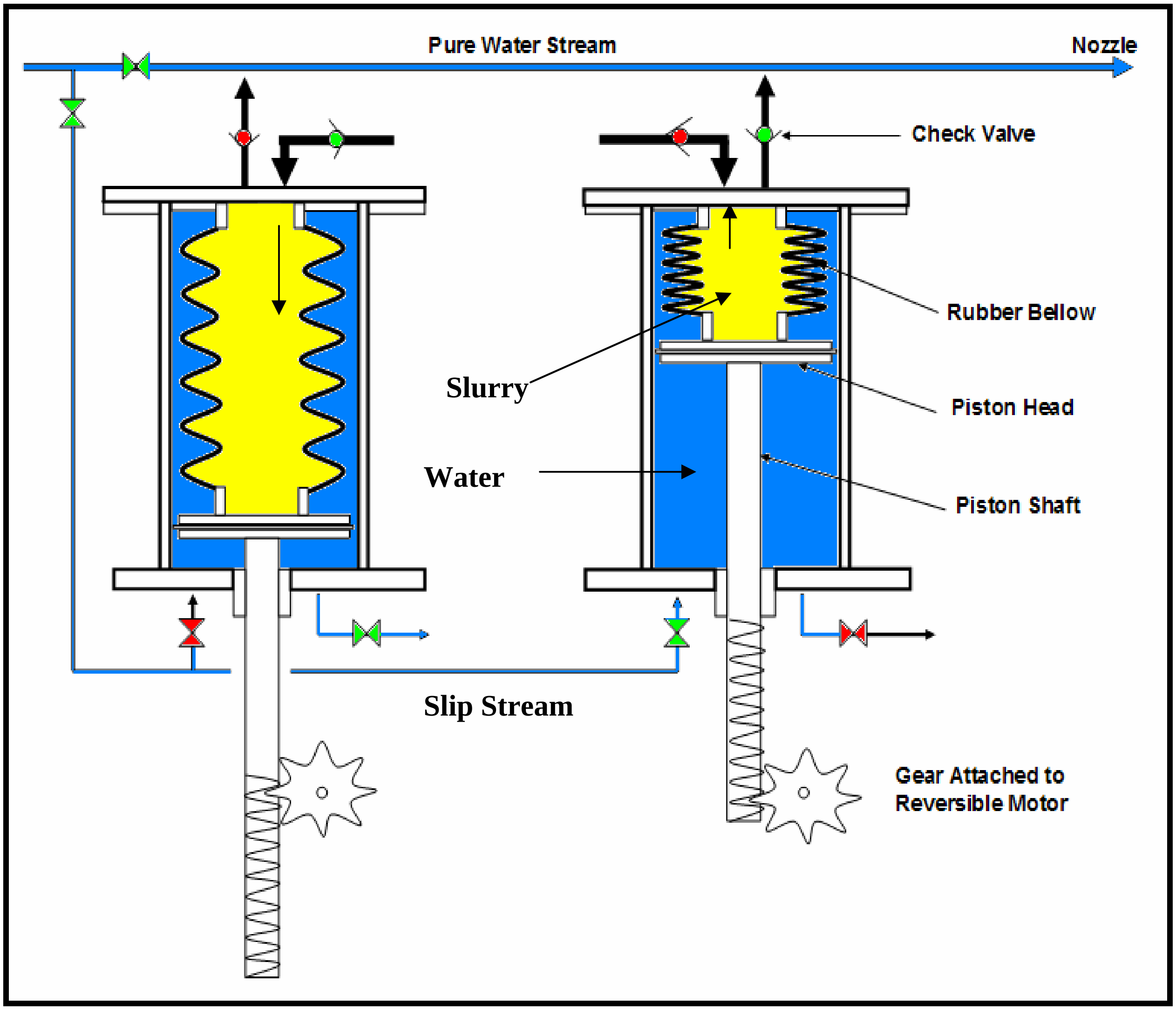

Figure 9 Schematic of Design I

The shaft forces the slurry contained in the bellow into the main high-pressure water stream. A slipstream provides force equilibrium across the piston and reduces the total load on the reversible motor. This arrangement still requires a slipstream, but would provide control over abrasive slurry injection rate by controlling the rpm of the reversible motor. It would take two such cylinder-motor combinations to accomplish continuous injection.

3.2.1 Process Description

Once the bellows are charged with slurry, opening the slipstream valves would pressurize the unit to mainstream pressure. Reversible motor would push piston upwards to begin injecting slurry to the main or pure water stream. Once the stroke is complete, closing the slipstream valves and bleeding pressure would allow the downward stroke. At the same time, the check valve on the slurry suction line would open in order to recharge the bellow.

3.2.2 Design Calculations for Design I

Force balance across the piston would yield,

$$F_1 = F_2 + F_{OP} \quad \text{---------------------------------} \ (3.1)$$

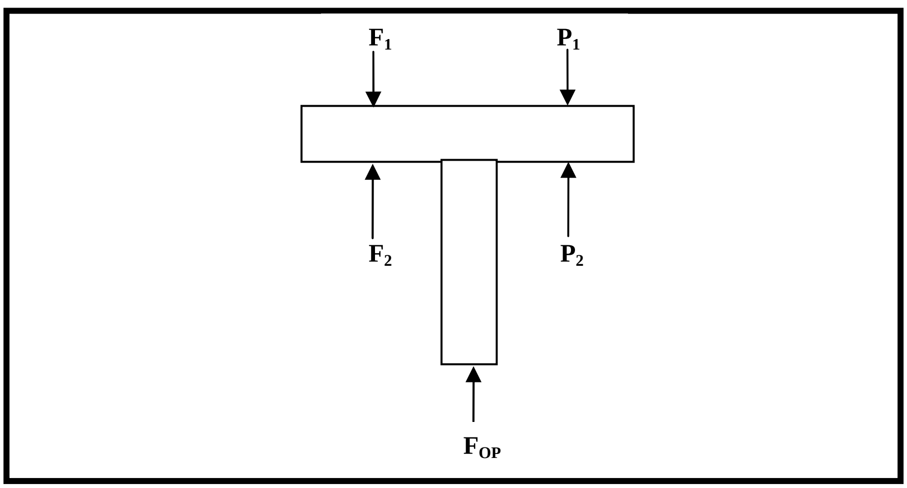

Figure 10 Force Balance Across Piston

$$F_1 = \frac{\pi}{4} \times D^2 \times P_1 \quad \text{-----------------------------} \ (3.2)$$

$$F_2 = \frac{\pi}{4} \times (D^2 - d^2) \times P_2 \quad \text{---------------------} \ (3.3)$$

Where, D is the piston diameter, d is the piston rod diameter and F_{OP} is the operating force required to push the piston and would essentially depend on the injection rate, but for simplicity it is assumed to be equivalent to the differential force across the piston as shown in Figure 10. Using Equation 3.1, 3.2, and Equation 3.3 in Equation 3.4

$$F_{OP} = F_1 - F_2 \quad \text{--------------------------------} \ (3.4)$$

$$F_{OP} = \frac{\Pi}{4} \times \left[D^2 \times (P_1 - P_2) + d^2 \times P_2 \right] \quad \text{-------} \ (3.5)$$

When $P_1 = P_2$,

$$F_{OP} = \frac{\Pi}{4} \times d^2 \times P_1 = \frac{\Pi}{4} \times d^2 \times P_2 \quad \text{------------} \ (3.6)$$

Let Q gal/min be the desired slurry injection rate, then; injection velocity would be given by,

$$V = \frac{Q}{2.448 \times D^2} \ \frac{ft}{\sec} \quad \text{-------------------------} \ (3.7)$$

Power required would be,

$$P = F_{OP} \times V \quad \frac{lbf \, . \, ft}{\sec} \quad \text{-------------------------} \ (3.8)$$

Required Horsepower for motor,

$$HP = \frac{P}{550} \quad \text{-------------------------------------} \ (3.9)$$

3.2.3 Limitations of Reversible Motor

Some serious concerns related to Design I are as follows:

1. The reversible motor can’t change the direction instantaneously; it needs to come to a full halt before any direction change.
2. If the check valve malfunctions the shaft would move down with velocity high enough to damage the gear and shaft arrangement.
3. Backlash associated with gear a gear system reduces power transmission efficiency.
4. Limited field applicability, as electricity is required to operate reversible motors.

3.3 Design II

Design II utilizes a hydraulic pump based external system to control the slurry injection rate, as shown in Figure 11.

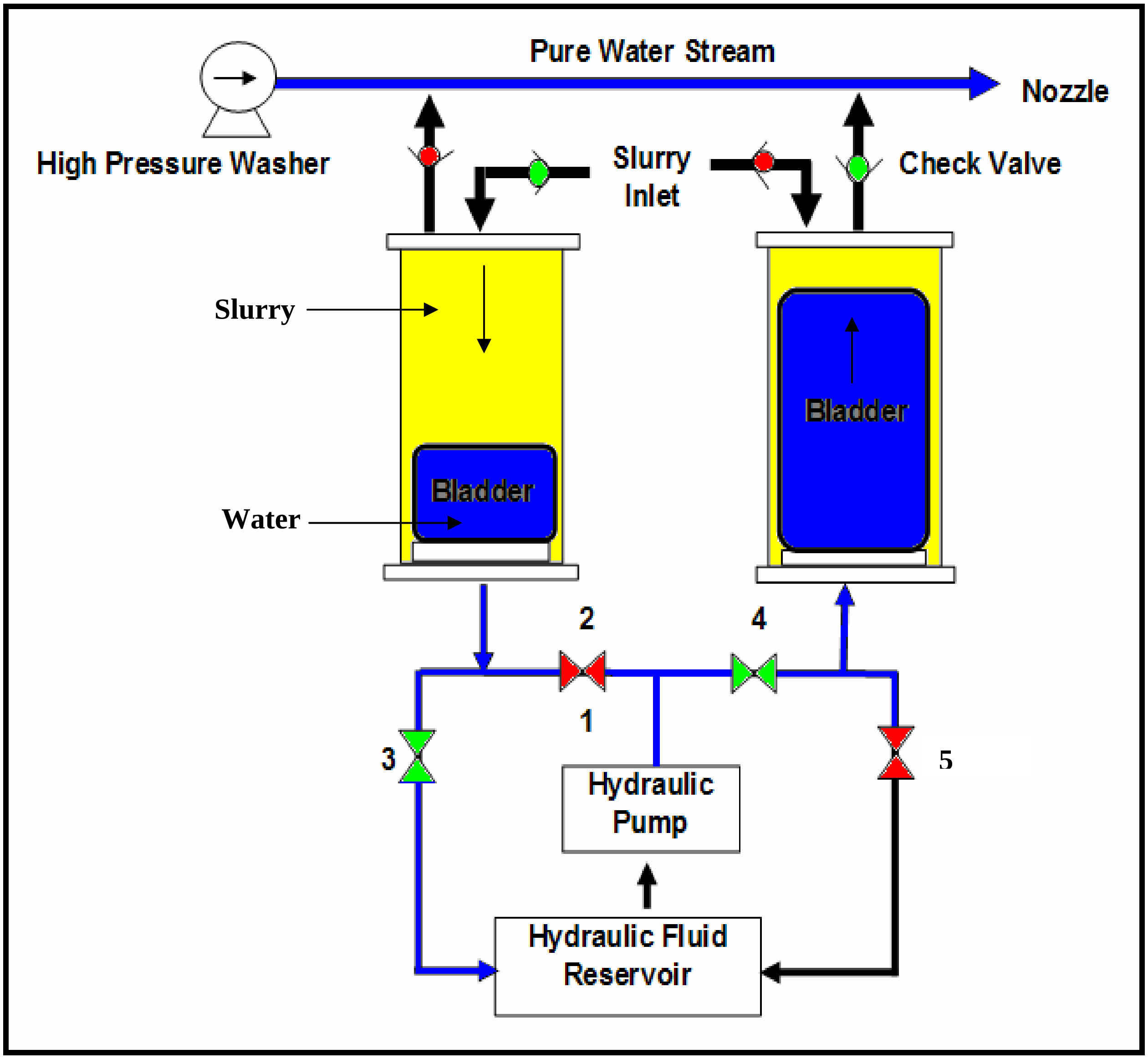

Figure 11 Schematic of Design II

In this design, a bladder contained in a high-pressure shell replaces the bellows. Slurry is charged to the shell side from pre-pressurized bulk storage tank and then injected into the high-pressure water stream by pressurizing bladder using a hydraulic pump. Varying hydraulic pump rate could control slurry injection rate. It would take two bladder units to make the process continuous. While one unit injects the slurry into the high-pressure water stream, the second unit recharges at the same time. The process can be automated by using solenoid valves in place of regular ball valves 1, 2, 3, 4 and 5.

3.3.1 Advantages of Design II over Design I

1. Eliminates the need of a reversible motor.
2. No gear arrangements or complex moving parts are required.
3. Piston rod and matching stuffing box are eliminated.
4. Hydraulic pumps are readily available.

Considering these advantages, Design II was assembled for testing with certain modifications as described in detail in Chapter 4. These modifications included, replacing the bladder assembly by the pressure accumulators and replacing hydraulic pump by a low power pressure washer.

CHAPTER 4: EXPERIMENTAL APPARATUS AND OPERATING PROCEDURE

The experimental apparatus for this study was assembled at Petroleum Engineering Training and Research Transfer Facility of Louisiana State University.

Experimental investigations were divided into two segments. First segment was to develop performance curves for a recently acquired 13-HP power pressure washer pump. These curves were later used in second segment (Design II Testing) for continuous and controlled slurry injection upstream of the nozzle. Further studies were carried out to investigate the effect of polymer on water jet performance and sand suspension ability. Three polymers namely, Xanthan, MF-55 (Polyacrylamide Emulsion), and CMC (CarboxyMethylCellulose) were used for this study. Kelco Oilfield Group donated Xanthan and MF-55. CarboxyMethylCellulose was available at LSU Well Facility.

4.1 Experimental Apparatus for Pump Performance Curves

Experimental apparatus to develop pump performance curves consisted of thirteen horse power gasoline engine powered pressure washer pump, three high pressure ball valves, one 5000 psig pressure gauge, a tachometer, a rotameter and essential piping. The apparatus was assembled as depicted in Figures 12 through 15. All the piping and fittings used for this experimental apparatus were rated for 3000 psig working pressure.

Pressure was regulated downstream of the pressure washer by operating the discharge valve. Flow rates were recorded using rotameter, as adjusting the rpm throttle varied engine rpm. Flow rate and rpm data were recorded for six different pressure settings, starting from zero psig to 2500 psig with, 500 psig increments. Pressure data was recorded using a pressure gauge which was mounted upstream of the discharge valve. A piece of reflecting tape was placed on the shaft connected to the fan of the pressure washer and tachometer was used, in optical mode, to measure engine rpm. Average engine rpm was recorded as the instantaneous tachometer readings fluctuated over a range of $\pm 10\%$.

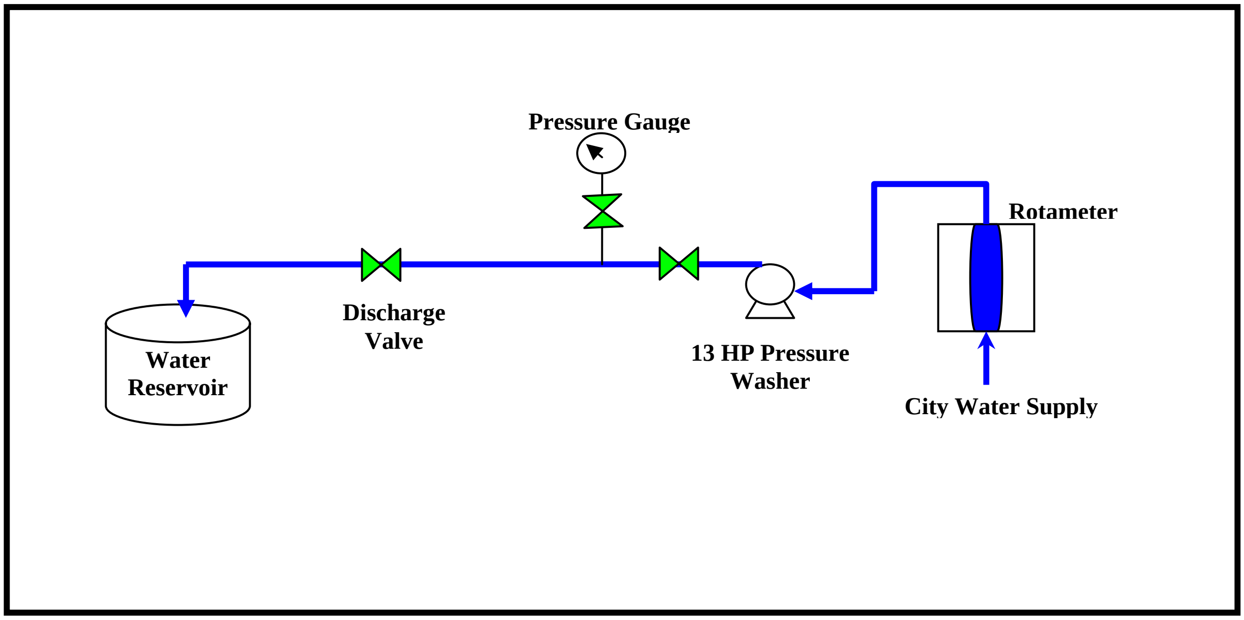

Figure 12 Schematic of Experimental Apparatus for Measuring Pump Performance Curves

Figure 13 Experimental Apparatus for Pump Performance Curves

Figure 14 Rotameter

Figure 15 Throttle to Control Engine RPM for 13-HP Pressure Washer

4.1.1 Experimental Procedure

The following procedure was followed to develop pump performance curves for pressure washer pump. It is critical to study pressure washer and tachometer operating manual before conducting experiments.

1. Assemble apparatus as depicted in Figure 12.
2. Make sure all the valves are open before starting the pump.
3. Set engine rpm to desired value by adjusting the throttle control.
4. Adjust discharge valve to get desired pressure reading on the gauge and let it stabilize. Closing the discharge valve yields more pressure build up upstream.
5. Read and record engine rpm using a tachometer.
6. Read and record flow rate from rotameter.
7. For next reading set throttle position towards higher engine rpm and repeat step (4) through step (6).

Data acquired from such experiments is recorded in Table A-1 in Appendix. The graphical representation obtained from this data was used to validate the flow rate readings obtained from rotameters.

4.2 Sand Suspension

Sand suspension ability of Xanthan, MF-55, and CMC was investigated by making 350 ml laboratory samples of varying concentration (w/w). Xanthan and CMC were available in powder form and needed lukewarm water for good mixing. MF-55 however was available in an emulsion form and was easily soluble in cold water. 50 grams of construction sand was added to each sample after the polymer hydrated in water and time for the sand to settle down was recorded.

4.2.1 Procedure

Following procedure was followed to make 1% (w/w) samples of the polymer. It is important to wear safety glasses while preparing samples.

1. Take 300 ml of water in a beaker.
2. Weight 3.5 grams of polymer.
3. Add polymer to water and mix well. It is advisable to use a mixer.
4. Add more water to bring the solution volume to 350 ml.
5. Let the sample stand for a while to release all the air that was entrained during mixing.
6. Add 50 grams of construction sand to the sample and mix again.
7. Put the slurry in a jar and fasten a lid on it.
8. Shake the slurry well and place the jar on a level surface.
9. Record the time, with a stopwatch, for the sand to settle down at the bottom of the jar.

Special precautions were taken while handling MF-55 solutions as it was very slippery and could cause serious hazards.

Table 2 Technical Data of Pressure Washers used in Experiments

Pressure Washer	Horsepower (HP)	Max. Output Pressure (PSIG)	Flow Rate @ Max. Pressure (GPM)	Engine RPM Control
1	5	2500	2.5	No
2	13	3700	4	Yes

4.3 Experimental Apparatus for Testing of Design II

Experimental apparatus for testing of Design II consisted of a gasoline engine driven pressure washer, two pressure accumulators, two rotameters, pressure gauges, one spool valve, and one eighty gallons spherical tank for bulk storage, a mixing tank, a centrifugal pump, essential piping, high pressure hoses, ball valves and fittings. The experimental apparatus was designed for a maximum working pressure of 3000 pounds per square inch, which included a safety factor of 1.6. The maximum working pressure for the apparatus was limited by a smaller pump (5 HP) as it was available on-site and could deliver 2.5 gallons of water at 2500 pounds per square inch and was used for main water stream. Table 2 provides some technical details of the pressure washers used in experimental apparatus.

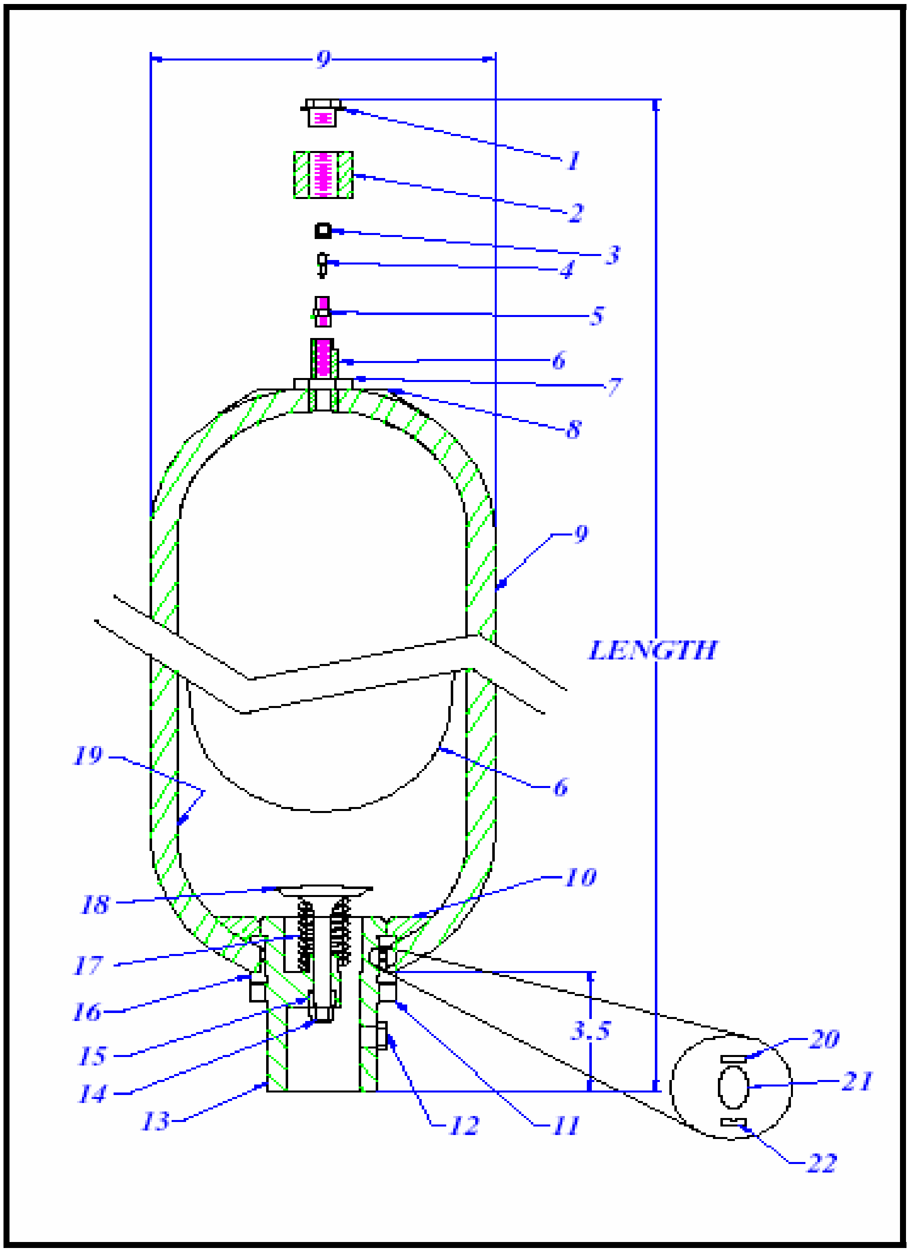

Figure 16 Pressure Accumulator (Source: www.accumulators.com)

Table 3 Parts Description of Pressure Accumulator (Source: www.accumulators.com)

Part Number	Description
1	Safety Cap
2	Protective Cap
3	Valve Cap
4	Valve Core
5	GT Gas Valve
6	Bladder Kit
7	Hex Jam Nut
8	Name Plate
9	Caution Label
10	Anti-Extrusion Ring
11	Locknut
12	Bleed Plug
13	Oil Port
14	Stop Nut
15	Piston
16	Spacer
17	Spring
18	Poppet
19	Shell
20	Metal Back-Up Ring
21	O-Ring
22	Rubber Back-Up Ring

4.3.1 Pressure Accumulators

Pressure accumulators served as critical components of the experimental apparatus used for high-pressure polymer injection. Figure 16 provides cross sectional view of a typical pressure accumulator. CAD Control Systems donated study two units of eleven gallons capacity each and maximum working pressure of 3000 psig for this study.

Both units were charged with polymer slurry on the shell side and, water was pumped inside the bladder using pressure washer pump with rpm control. The bladder provided an impermeable barrier between polymer slurry and water, preventing any dilution of the polymer slurry before the injection point. This would be critical if polymer slurry consisted of suspended sand. Significant dilution could cause the sand to settle out permanently and block flow lines, thus causing serious safety hazards.

4.3.2 Description of Apparatus

The components were assembled as per the schematic depicted in Figure 17 whereas a photograph of the actual experimental apparatus is shown in Figure 18. Smaller pressure washer (5-HP) was used to deliver water (2.5 gallons per minute) straight to the nozzle and this stream is referred to as main water stream. Polymer solution (1% w/w) was prepared in the mixing tank and was pumped to the bulk storage tank where it was pressurized by compressed air to pressure level between 100 psig to 130 psig. Pressure accumulators were charged from bottom with pressurized polymer solution by operating appropriate valves. Water from the large power pressure washer was pumped into the bladder of either of the pressure accumulator by moving the lever of directional control spool valve. Adjusting RPM throttle of 13-HP pressure washer controlled water flow rate pumped into the bladder. Polymer solution was injected into the main water stream, upstream of the nozzle by the expanding bladder.

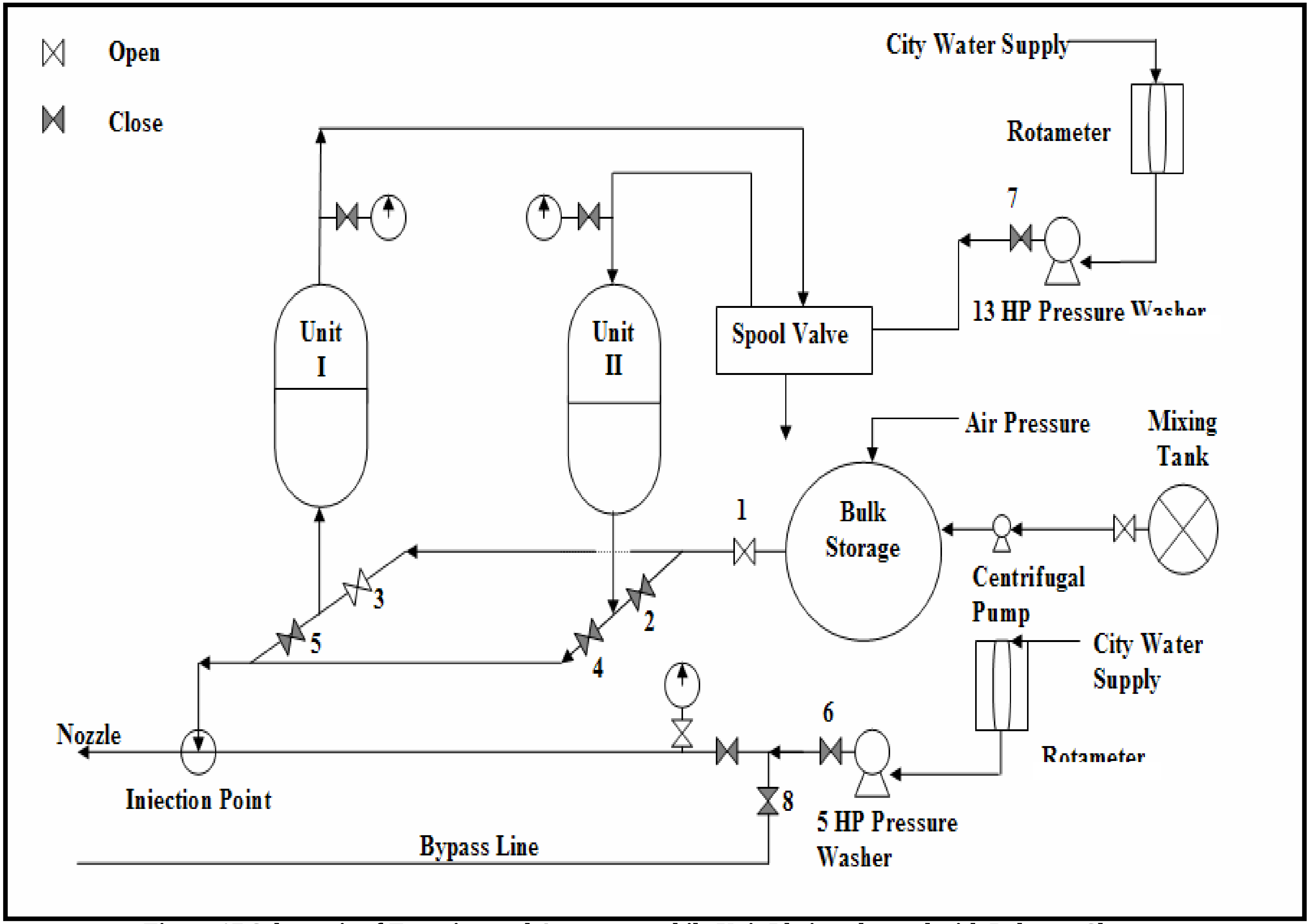

Figure 17 Schematic of Experimental Apparatus while Unit I being charged with Polymer Slurry

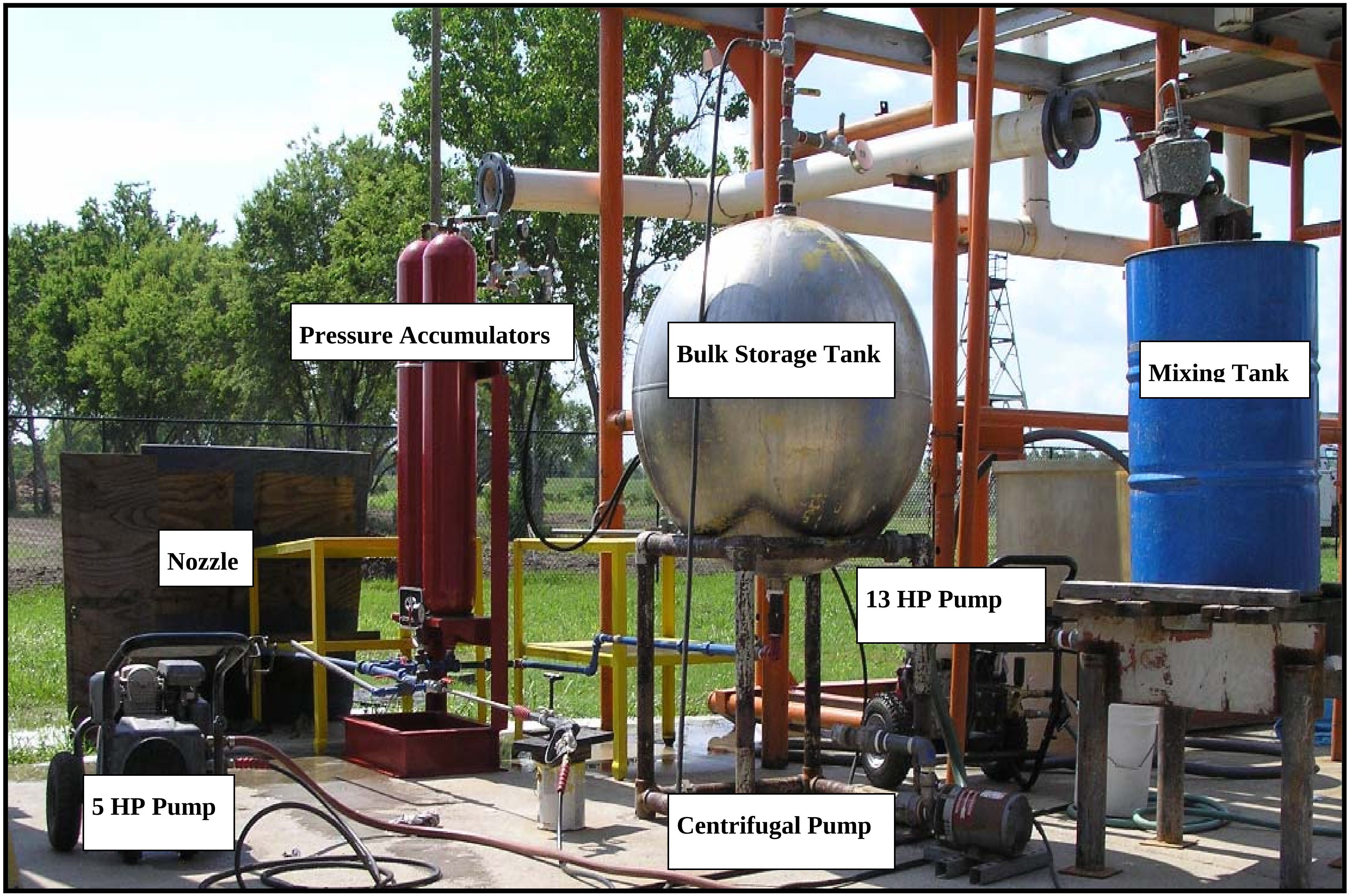

Figure 18 Experimental Apparatus used for Design II Testing

4.3.3 Safety Considerations

To ensure proper safety the experimental apparatus was equipped with safety relief valves and bypass lines. The directional control spool valve used was equipped with pre-installed safety relief valve with an adjustable range from 1500 psig to 3000 psig and was set at 2500 psig for our experiments. Although, the storage tank was rated for 3000 psig working pressure, but still another spring loaded safety relief valve set at 150 psig was mounted on it to avoid over pressurizing the Schedule-40 recharging line, in case of pressure leakage while polymer was being injected into the high pressure water stream. Recharging lines were equipped with 3000 psig rated check valves just upstream of the pressure accumulators. Main water stream was equipped with a bypass line upstream of the injection point.

4.3.4 Experimental Procedures

Experimental procedures for the recharging cycle, in which accumulators were charged with polymer solution from bulk storage and for the injection cycle, in which polymer solution was injected into main water stream, are written in Section 4.3.4.1 and Section 4.3.4.1, respectively.

4.3.4.1 Operating Procedures for Charging Cycle

Following procedure was used while charging the pressure accumulators with polymer solution from pressurized bulk storage tank as illustrated in Figure 17.

1. The bulk storage tank is filled with polymer solution and is pressurized to100 psig minimum, to overcome the friction in recharging lines and to open the check valve.
2. To charge pressure accumulator unit I, open valve-1 and valve-3 and move the spool valve lever accordingly. While doing so make sure valve-2 and valve-5 are closed.
3. To charge pressure accumulator unit II, close valve-3 and valve-4, and open valve-2.
4. Move spool valve lever in appropriate direction and close valve-2.

4.3.4.2 Operating Procedure for Injection Cycle

Figure 19 and the following operating procedures were followed to inject polymer solution from pressure accumulators to the high-pressure water stream.

1. Connect rotameters suction hose to both pressure washer and make sure the water supply is on. Connect the 5-HP pressure washer outlet to valve-6, and, connect 13-HP pressure washer outlet to spool valve inlet.
2. Close valve-9, valve-4, and valve-5 and open valve-6 and valve-8.
3. Power up the smaller pressure washer (5-HP), open valve-9 and slowly close valve-8. This step would deliver pure water stream to the nozzle. Record the reading on main water stream pressure gauge.
4. Power up the 13-HP pressure washer and set the throttle at desired engine rpm leaving the spool valve lever in neutral position.
5. To inject the polymer solution from pressure accumulator unit I move the spool valve lever in appropriate direction. Keep a keen watch on pressure gauge-2 and bring the spool valve lever in neutral position once the reading on gauge-2 is a little more than gauge-1.
6. Open valve-5 and move the spool valve lever to the previous position.
7. Record the readings of pressure gauge-1, pressure gauge-2 and both rotameters.
8. Take pictures of the jet as it emerges out of the nozzle.
9. Once the pressure accumulator unit I has pumped all the polymer solution the reading on pressure gauge-2 would increase rapidly. At this point bring the spool valve lever to neutral position and close valve-5.
10. To inject polymer solution from unit II, follow step (5) through step (9).
11. While unit II is injecting, unit I could be charged simultaneously by opening valve 3.

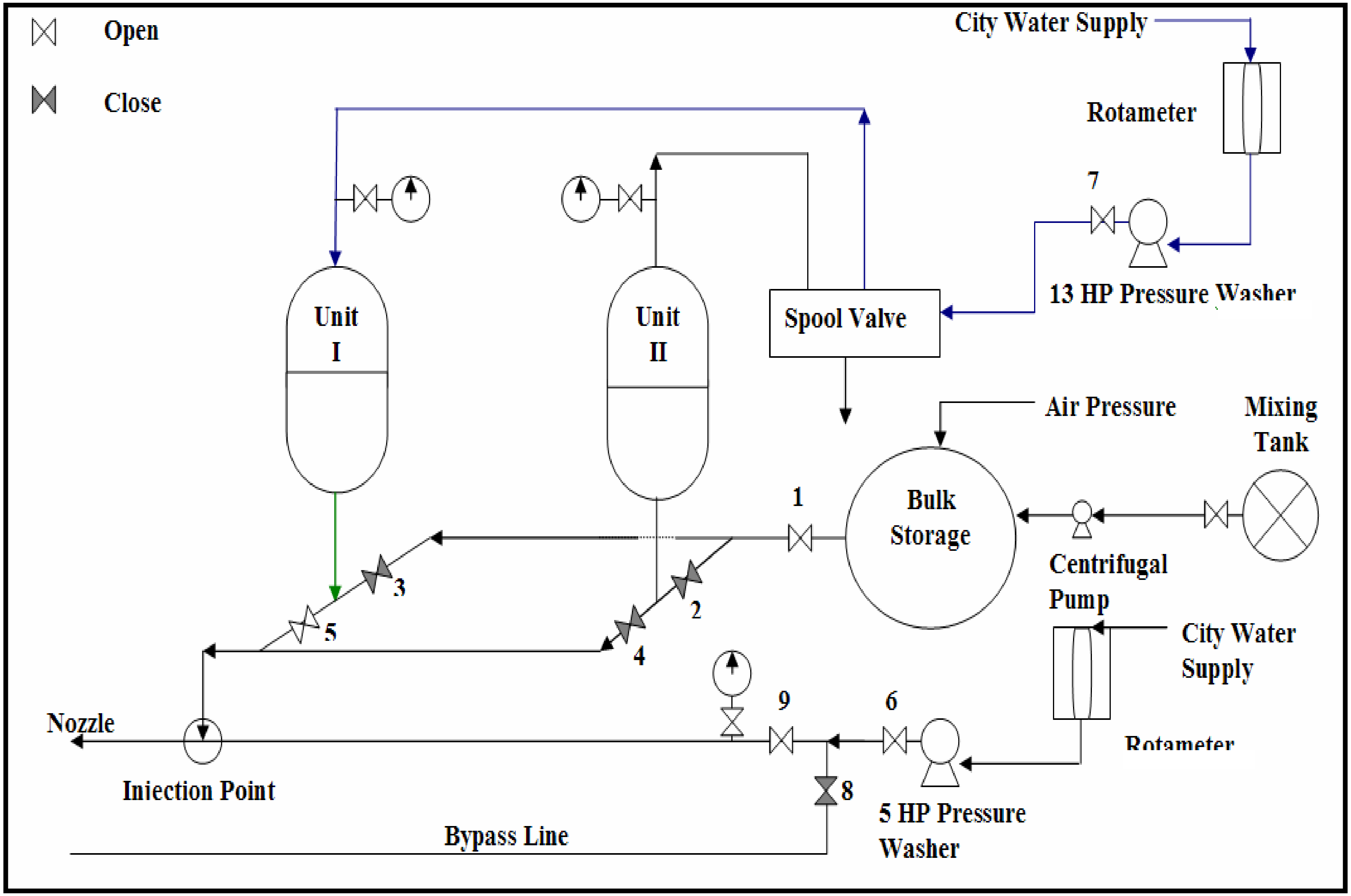

Figure 19 Schematic of Experimental Apparatus while Unit I is injecting Polymer Slurry

CHAPTER 5: EXPERIMENTAL RESULTS

Following the procedure illustrated in Chapter 4, and using experimental apparatus depicted in Figure 12, flow rate data were recorded as a function of engine rpm and pressure. From these data (Table A-1), variation of flow rate Characteristics of pressure washer pump with engine rpm and downstream pressure are plotted in Figure 20.

The objective of this study is to develop a slurry injection that allows injection of slurry into a water jet at a controllable constant rate. The ability of our apparatus to do so was evaluated by injecting various polymer slurries and visually observing their impact on the performance of water jet. This is accomplished by using experimental apparatus as depicted in Figure 18, and graphical representation were developed from the data (Table A-3) obtained by processing jet images using GIMP® (Image Processing Software).

Even though the system could inject slurry at constant rate, final concentration in solid laden slurry would change if the solid settles out of slurry. The ability of different polymer to suspend sand was studied by making samples of varying polymer concentrations and results are detailed in Figures 26 through 29.

The smaller pressure washer (5-HP) constrained the experimental pressures to stay below 2500 psig and polymer flow rate to stay below 3.5 gallons per minute for 0.069 inches nozzle. Considering the allotted budget, experiments were conducted within the limits of 2500 psig pressure and polymer injection rates were varied from two gallons per minute to 3.5 gallons per minute.

5.1 Pump Performance Characteristics

In order to study the effect of downstream pressure on pump performance, flow rates were recorded as engine rpm was varied at six pressure levels, ranging from Zero psig to 2500 psig with 500 psig increment. Measured data were plotted as shown in Figure 20. Flow rate data were obtained using a rotameter connected to the suction line of the pump and engine rpm was recorded using a tachometer. Average engine rpm was used as tachometer readings fluctuated over a range of $\pm 10\%$. Recorded data is tabulated in (Table A-1).

An immediate observation that could be made from Figure 20 is that flow rate varies linearly with engine rpm. However, the slope tends to decreases as downstream pressure increases. Hence, at a constant engine rpm the pump is able to deliver less fluid at higher pressures. In order to maintain hydraulic horsepower constant, flow rate would decrease according to Equation 5.1.

$$Hydraulic\ Horsepower = \frac{P \times Q}{1714} \text{ ----------------------------(5.1)}$$

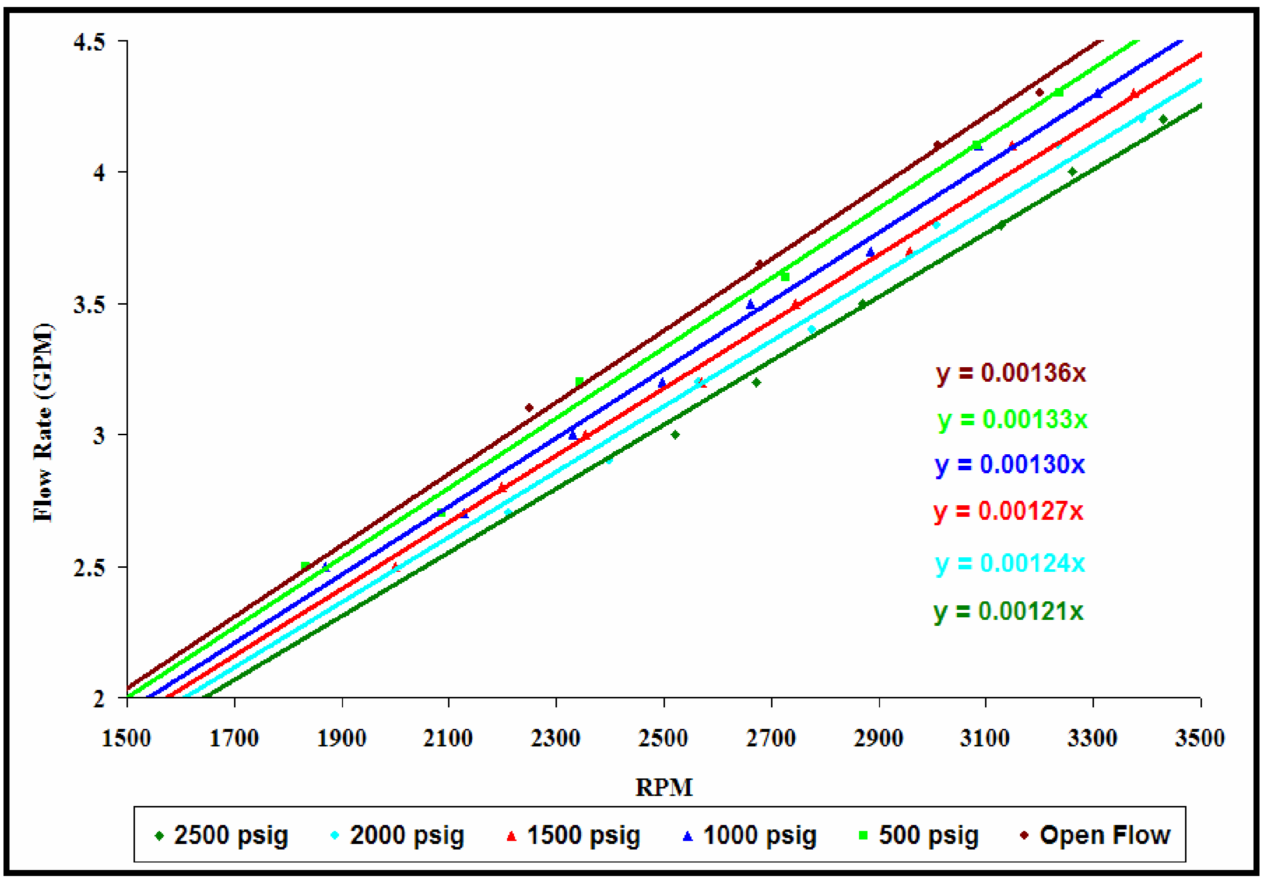

Figure 20 Thirteen Horsepower Pressure Washer Pump Performance Curves

Where, Q is the flow rate and P is the pressure. The isobaric lines in Figure 20 can be represented by a linear equation,

$$Q = m(RPM) + C \quad \text{---} (5.2)$$

Where, m is the slope and C is the intercept. Technically, at zero rpm flow rate would be zero. Hence, for all isobaric lines the intercept is set at the origin. So, the equation of interest would be,

$$Q = m \times RPM \quad \text{---} (5.3)$$

The slope of the isobaric lines is recorded in Table 4, is used to generate Figure 21 to determine the relationship between pressure and slope of the isobaric lines as described by Equation 5.4.

$$m = (-6.0 \times 10^{-8})\Delta P + 1.36 \times 10^{-3} \quad \text{------------------------------} (5.4)$$

Table 4 Slopes of Isobaric Pump Performance Curves

Pressure (PSIG)	**Slope** ($\frac{dQ}{dRPM}$)
0 (Open Flow)	1.36×10^{-3}
500	1.33×10^{-3}
1000	1.30×10^{-3}
1500	1.27×10^{-3}
2000	1.24×10^{-3}
2500	1.21×10^{-3}

Using Equation 5.4 in Equation 5.3 gives a relation between engine rpm, flow rate, and differential pressure and is given Equation 5.5

$$Q = [(-6.0 \times 10^{-8} \times \Delta P) + 1.36 \times 10^{-3}] \times RPM \quad \text{---------------} \quad (5.5)$$

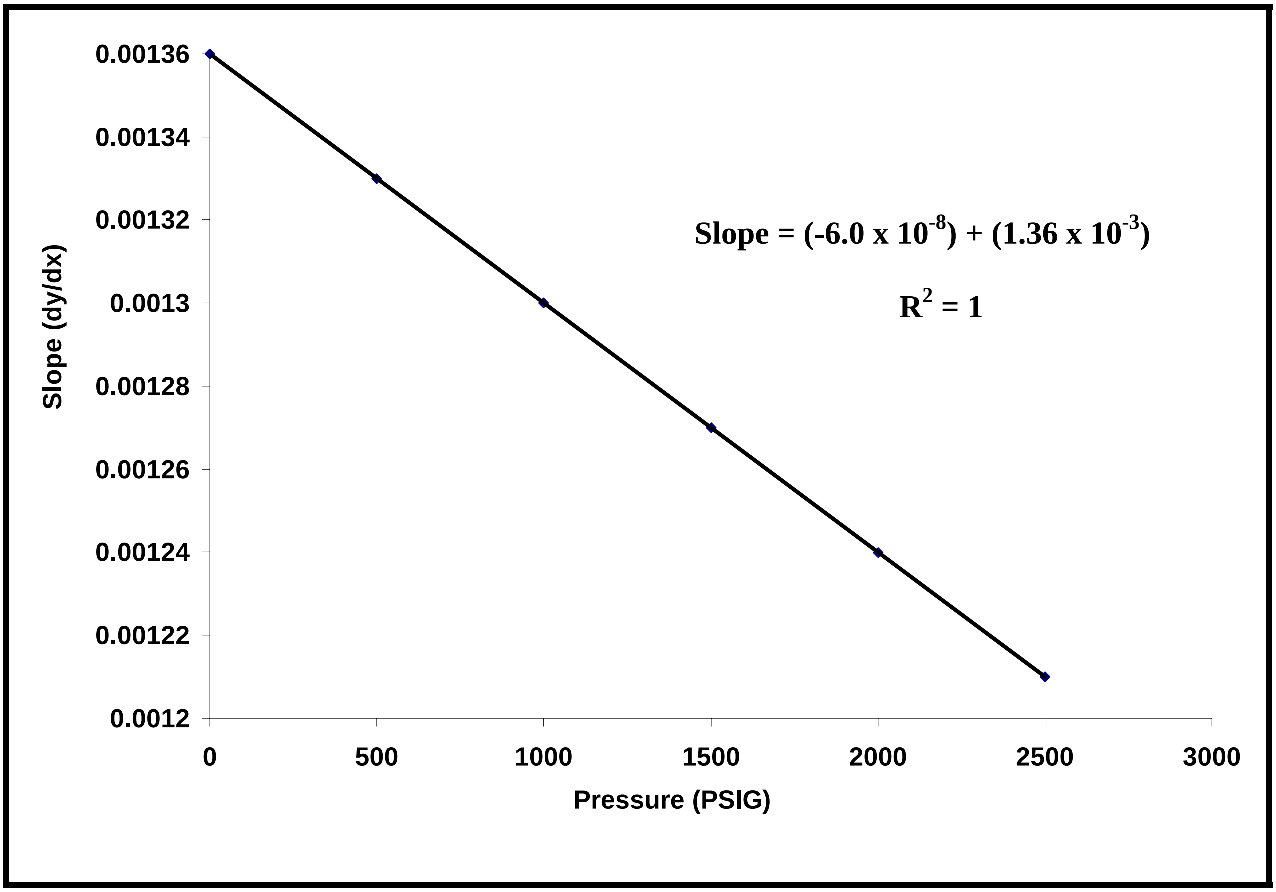

Figure 21 Effect of Pressure on Slope of Isobaric Lines

Equation 5.5 is good for 13-HP pressure washer, used in conducting experiments, but similar equation could be generated for any reciprocating pump. Figure 20 and Equation 5.5 were used during the testing of Design II to vary polymer injection rate. If downstream pressure is known, Equation 5.5 could be used to set pump rpm to achieve the desired flow rate. The flow rate data generated from Equation 5.5 is reported in Table A-2 of Appendix. This data was plotted against the measured flow rate as depicted in Figures 22 through 25, to examine the accuracy of results. All measured values stayed with in 5% error window of the calculated data.

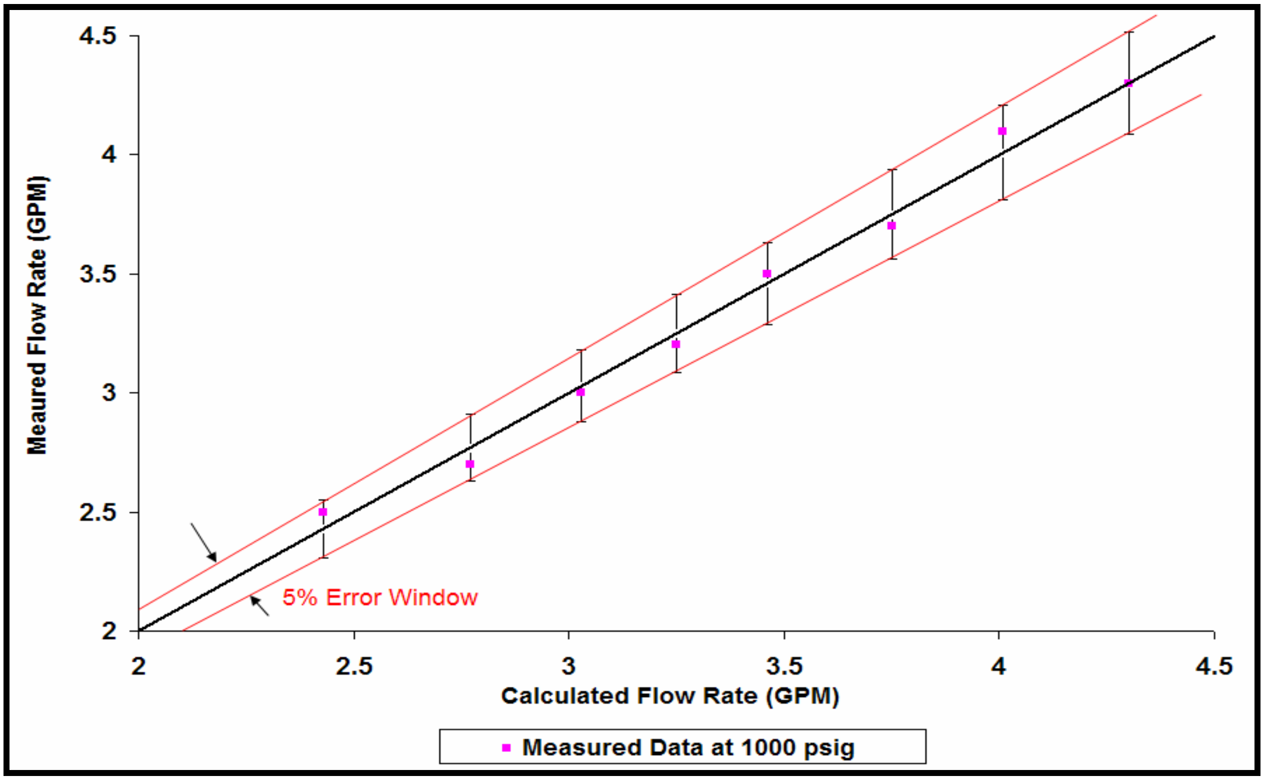

Figure 22 Comparison between Calculated and Measured Flow Rate at 1000 psig

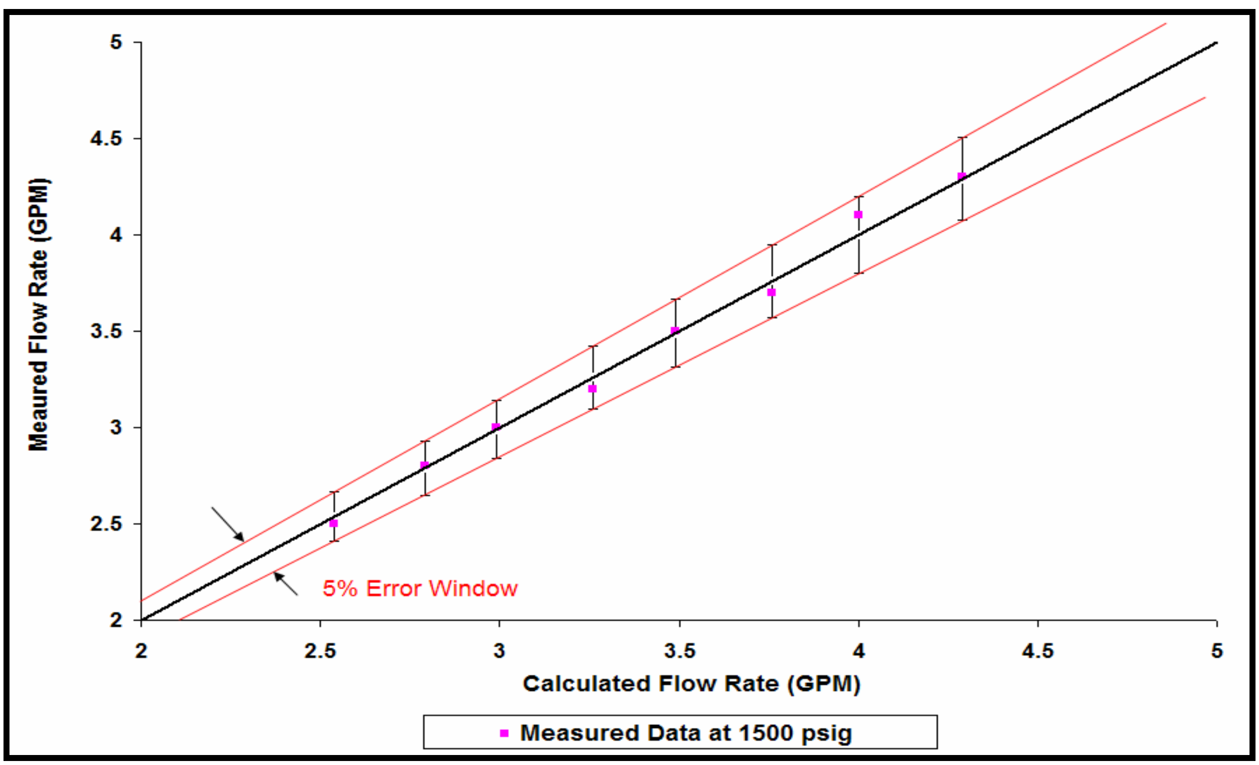

Figure 23 Comparison between Calculated and Measured Flow Rate at 1500 psig

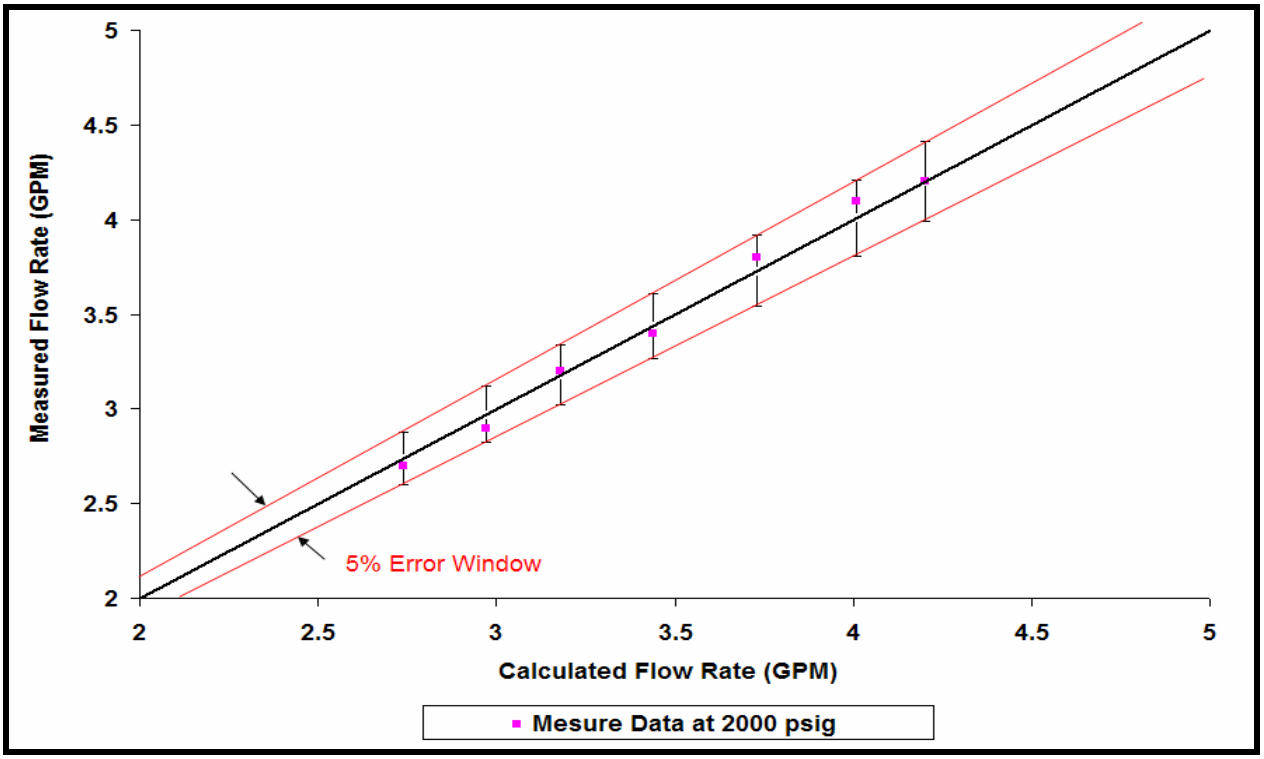

Figure 24 Comparison between Calculated and Measured Flow Rate at 2000 psig

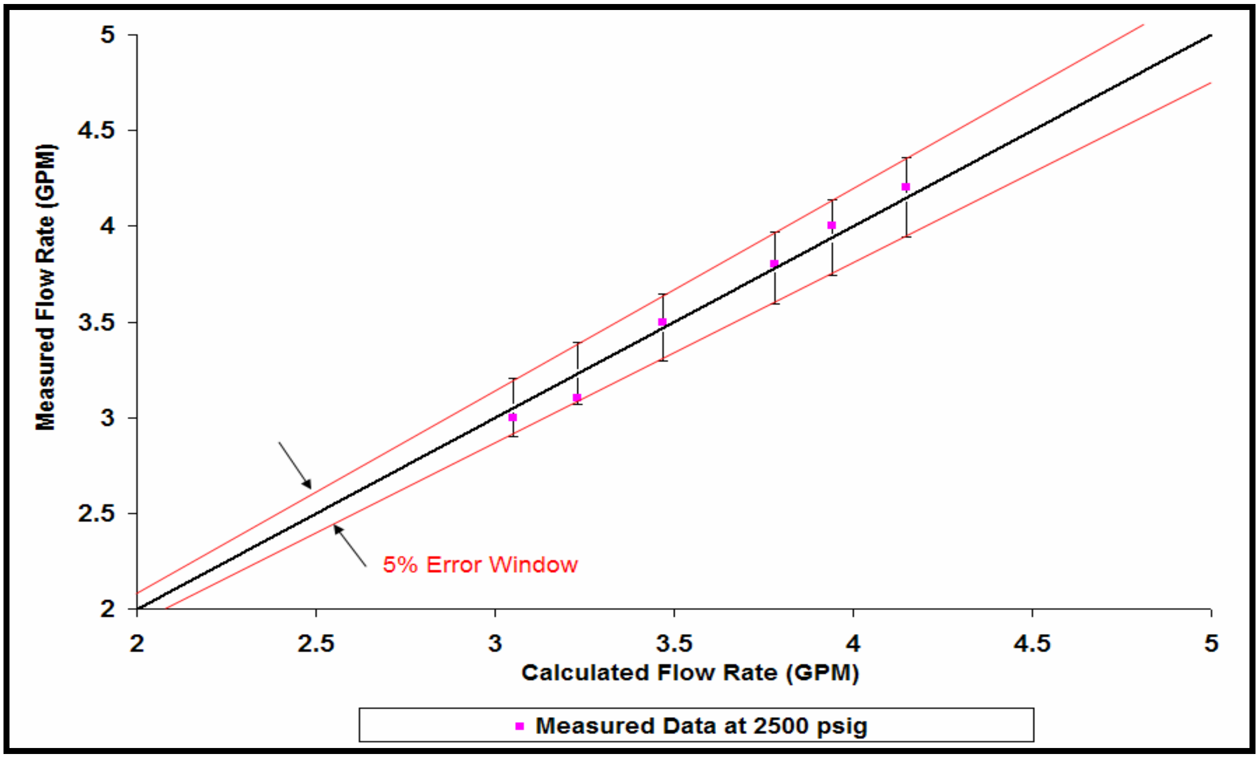

Figure 25 Comparison between Calculated and Measured Flow Rate at 2500 psig

5.2 Slurry Suspension

Three different polymers, namely, Xanthan, MF-55 (Polyacrylamide Emulsion), and CMC (CarboxyMethylCellulose) were analyzed for sand suspension competence in Figures 26 through 29. 350 ml samples of polymer dispersions of different concentration were prepared and 50 grams of construction sand was suspended in each of them. Time for the sand to settle to the bottom was recorded using a stopwatch and is tabulated in Table 5.

Table 5 Settling Time of Sand in Different Polymer Solution

Polymer	Concentration (%)	Amount of Sand (Grams)	Sand Settling Time
Xanthan	0.25	50	20 seconds
Xanthan	0.38	50	20 seconds
Xanthan	0.44	50	60 minutes
Xanthan	0.50	50	150 minutes
Xanthan	0.63	50	Didn’t Settle after 1 week
Xanthan	0.75	50	Didn’t settle after 1 week
Xanthan	1	50	Didn’t settle after 1 week
Xanthan	1	150	Didn’t settle after 1 week
MF-55	2	50	20 seconds
MF-55	5	50	5 minutes
CMC	6.5	50	20 seconds
CMC	7	50	20 seconds
CMC	7.5	50	60 seconds

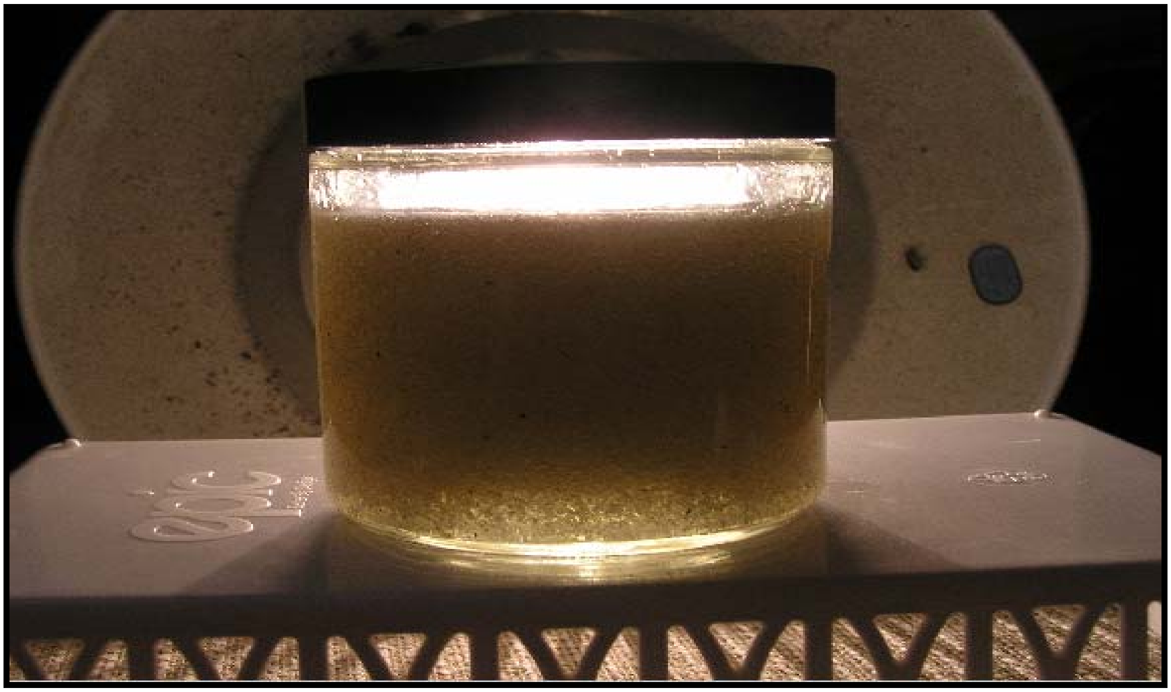

Figure 26 Sand Suspension in Xanthan (1% w/w) After One Week

Figure 27 Sand Suspension in Xanthan (0.50% w/w) After 120 Minutes

Figure 28 Sand Suspension in MF-55 (5% W/W) After Five Minutes

Figure 29 Sand Suspension in MF-55 (3% w/w) After Sixty Seconds

Xanthan samples at concentration higher than 1 % (w/w) were too viscous to handle with available equipments. Dispersions of MF-55 at concentrations less than 1% (w/w) could not hold sand in stable suspension for any length of time. CMC dispersions below 6.5% (w/w) concentration did not hold sand and became too viscous at concentration above 7.5% (w/w). Considering the viscosity of CMC it was not used for testing Design II.

5.3 Effect of Polymers on Water Jet Performance

The effect of Xanthan Gum and MF-55 on improving water jet performance was studied. All of these experiments were conducted by following the procedure as illustrated in Section 4.2 of Chapter 4. Pressure accumulator bottles were charged with pre-pressurized polymer from bulk storage tank. The polymer dispersion at 1% (w/w) concentration was then injected into main water stream at a controlled rate by inflating the accumulator bladder using 13-HP pressure washer. Images of the jet as it emerged out of the nozzle were processed to determine the length of the jet using an image processing software, GIMP®.

Length of the water jet was measured from the point it exits the nozzle to the point where its diameter became twice the diameter of the exit stream and this length was used as one of the parameters to analyze the effect of different polymers on water jet. To make the comparisons realistic and reasonable polymer streams were compared with the base case where only water shoots through the nozzle. Figures 30 through 35 show the images of jet for five gallons per minute of flow with 0.5% (w/w) polymer concentration through 0.069 inches diameter nozzle captured and processed for edge detection. Flow rate data for experiments conducted to obtain these figures is recorded in Table 6. Pictures were taken as jet emerged from the nozzle. Sobel edge detection option in GIMP® was used to process all images. Detailed data is reported in Table A-3 through Table A-7.

Table 6 Experimental Parameters for the Test Run

Nozzle Diameter (inches)	0.069
Water Stream Flow Rate (GPM)	2.5
Polymer (1% w/w) Injection Rate (GPM)	2.5
Total flow through nozzle (GPM)	5
Polymer concentration in water jet (w/w)	(2.5/5) x 1% = 0.5%

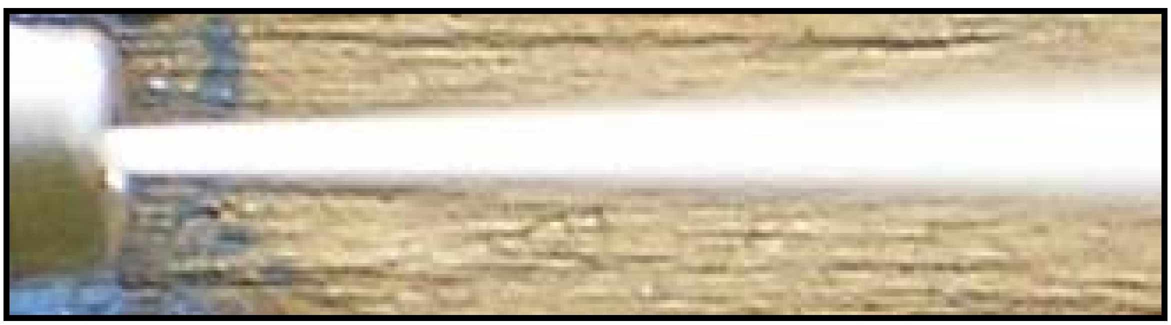

Figure 30 Image of Water Jet at Five Gallons per Minute

Figure 31 GIMP Processed Image of Water Jet at Five Gallons per Minute

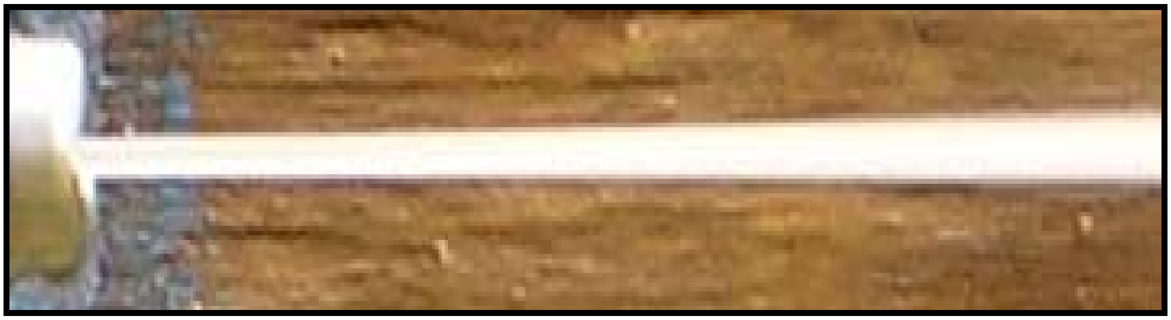

Figure 32 Image of Water Jet with 0.50% Xanthan

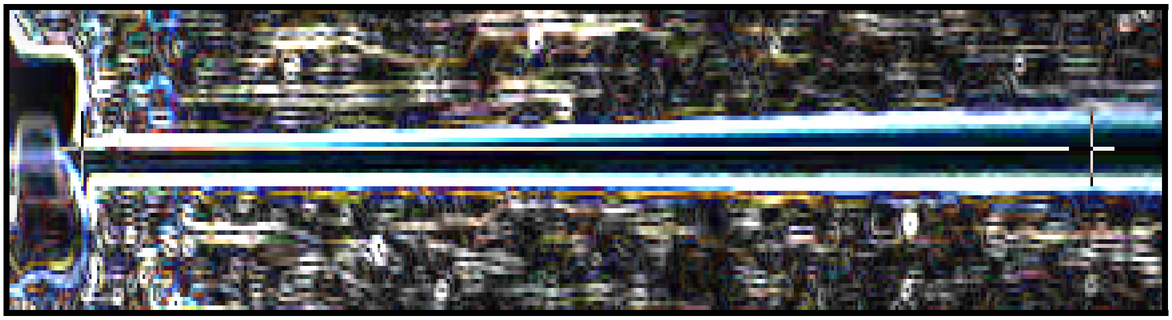

Figure 33 GIMP Processed Image of Water Jet with 0.50% Xanthan

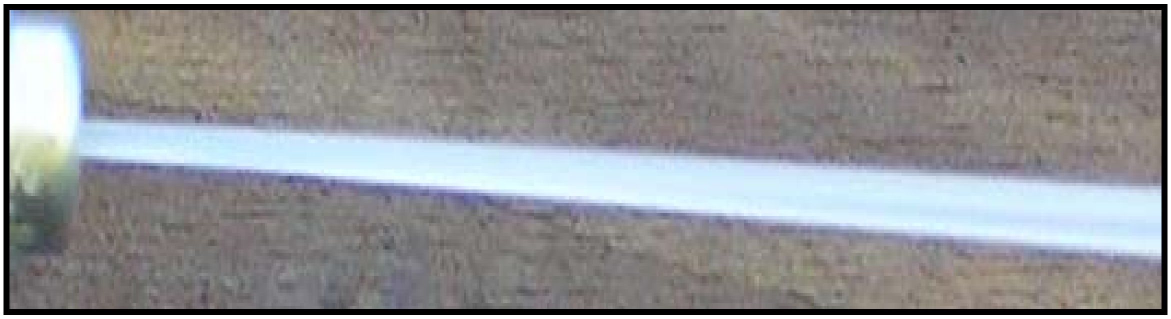

Figure 34 Image of Water Jet with 0.50% MF-55

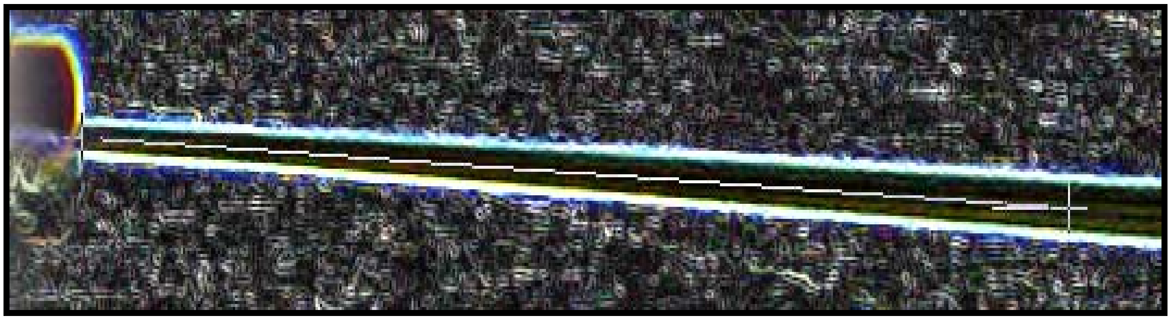

Figure 35 GIMP Processed Image of Water Jet with 0.50% w/w MF-55

Similar images were obtained as polymer concentration was varied in the main stream. Measured jet length for each run was recorded in Table A-3 of the Appendix. This data was used to develop graphical representation as depicted in Figure 36, to study the effect of polymer concentration on jet length.

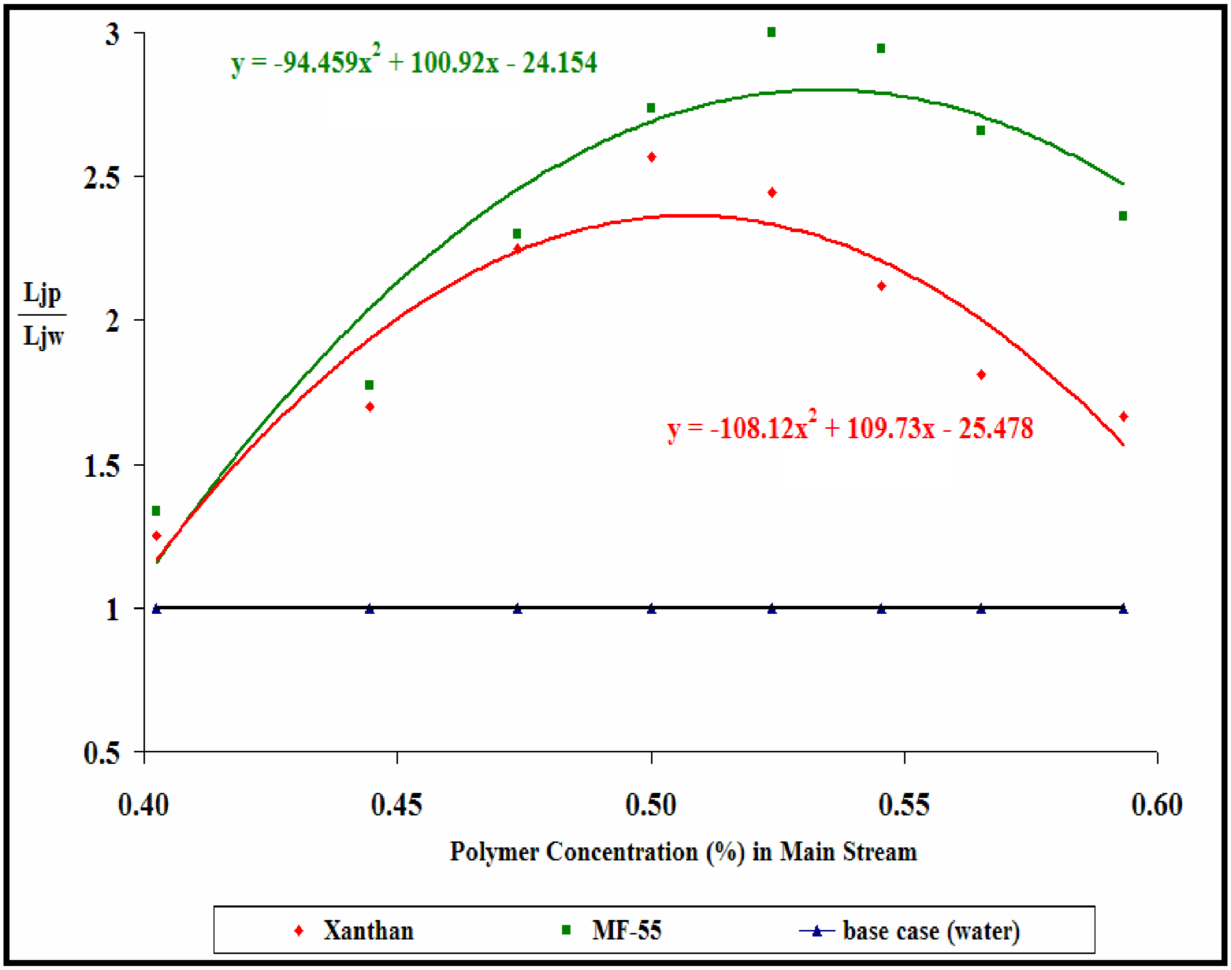

Figure 36 Relation between Jet Length and Polymer Concentration

The Y-axis of the plot refers to the ratio of jet-length obtained using polymer slurry, compared to the jet-length obtained with water. Polymer concentration in mainstream was calculated using relation as described in Equation 5.6 and the term "Loading Ratio" used in this discussion was described as the amount of polymer injected per gallon of water.

$$Main\ Stream\ Conc. = \frac{Polymer\ Slurry\ Flow\ Rate}{(Water\ Flow\ Rate + Polymer\ Slurry\ Flow\ Rate)} \times Bulk\ Slurry\ Conc. \text{-(5.6)}$$

$$Loading\ Ratio = \frac{Polymer\ Slurry\ Flow\ Rate}{Water\ \ Flow\ Rate} \text{ ----------------------(5.7)}$$

One immediate observation that could be made from Figure 36 is that for Xanthan and MF-55 initially jet length increased with increasing loading ratio and polymer concentration, but than started decreasing with any further increase in polymer concentration. The maximum point for Xanthan was recorded at a concentration of 0.50% w/w, while for MF-55 it was recorded at 0.52% w/w concentration.

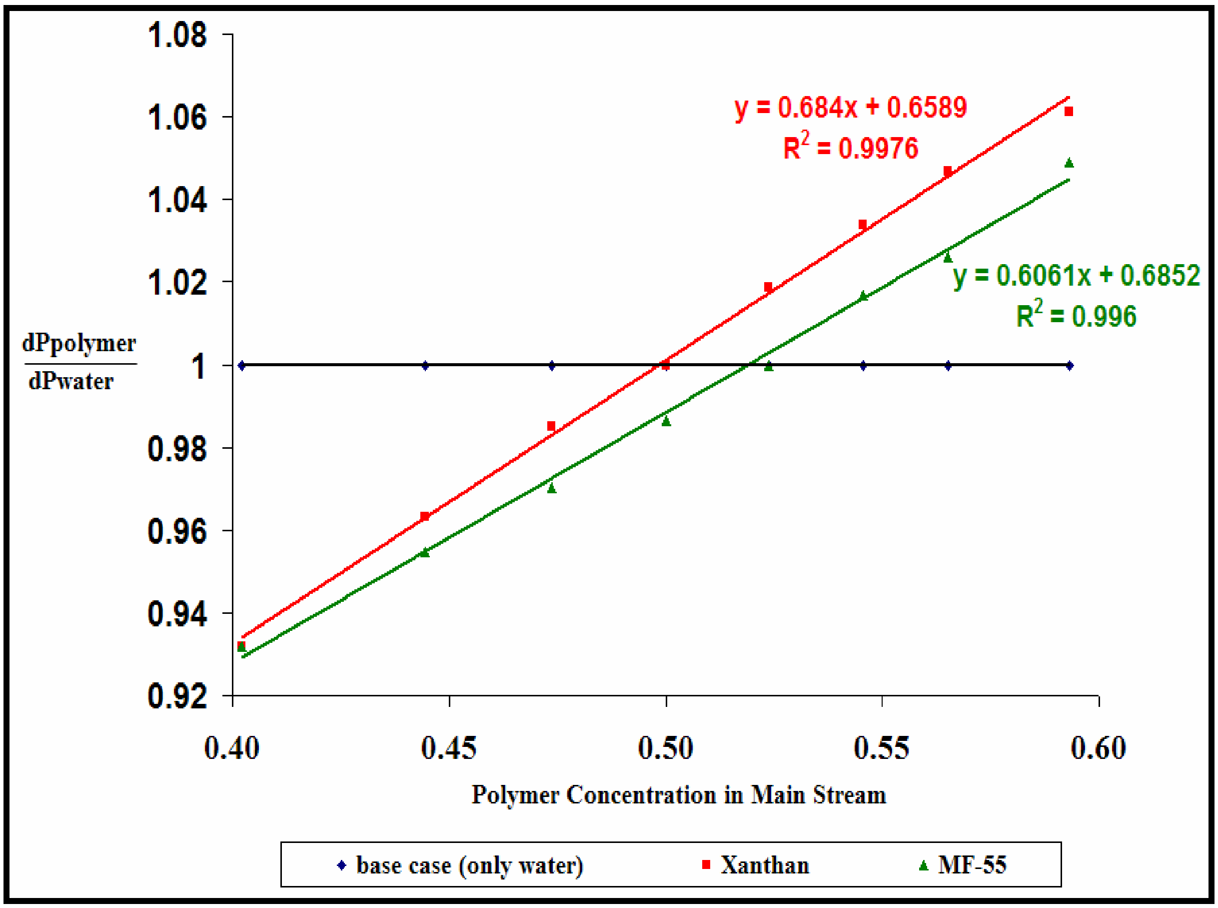

Figure 37 Pressure Requirement for Flow through 0.069 inches Diameter Nozzle

Pressure was recorded upstream of the injection point for water, Xanthan, and MF-55 run while the loading ratio was varied. The data is reported in Table A-4 in Appendix. This data was used to develop the graphical representation as depicted in Figure 37 showing the relationship between pressure drop and flow rate through the nozzle.

Total flow rate through 0.069 inches tungsten carbide nozzle was used to develop Figure 37; hence it consisted of flow rates of both main water stream and the flow rate coming from pressure accumulator bottles. Since the pressure used here was recorded upstream of the injection point it did not include any pressure losses across the pressure accumulator bottle. Xanthan reduced the pressure requirement until the flow rate through the nozzle reached approximately five gallons per minute i.e. a loading ratio of one. However, further increase in loading ratio increased the pressure requirement. MF-55 followed the same trend and started increasing pressure requirement once loading ratio reached 1.1.

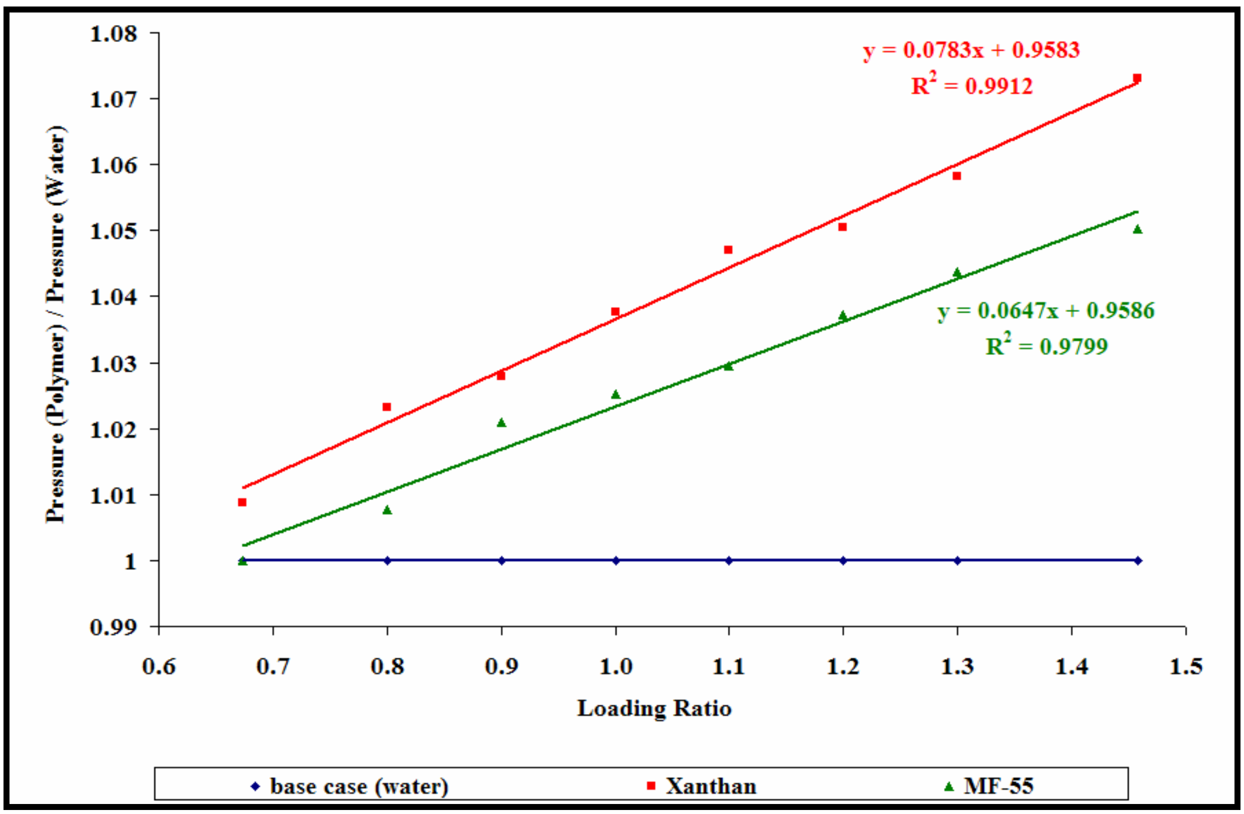

Figure 38 Pressure Drop across Pressure Accumulator at Varying Injection Rate

To examine the pressure drop across pressure accumulators Figure 38 was developed using the data from Table A-5, Table A-6, and Table A-7 of Appendix. Xanthan being most viscous at 1% concentration, among the polymers used, required highest pressure for same flow rate. The pressure was recorded from the gauge, which was mounted on top of the accumulators.

5.4 Economic Analysis

An economic analysis was done on Xanthan, MF-55, and CMC. Sand suspension ability was the criteria set for this analysis. Dispersion of Xanthan at 0.75% concentration by weight suspended 50 grams of construction sand for approximately a week, whereas, dispersion of MF-55 suspended sand for less than a minute at 5% concentration by weight while CMC suspended same amount for sand for 30 minutes at 7.5% concentration by weight. Price per pound recorded in Table 7 was obtained from Kelco Oilfield Group.

Table 7 Economic Analysis of Polymers used in Experiments

Polymer	Concentration (%)	Quantity (lb/bbl)	Price/LB $	Total Price $/bbl
Xanthan Gum	**0.75**	**2.625**	**4.93**	**12.94**
MF-55	**5**	**17.5**	**0.97**	**16.98**
CMC	**7.5**	**26.25**	**1.25**	**32.80**

Based on Table 7, even though Xanthan is the most expensive on per pound basis, among the three candidate polymers it would still be the most economical polymer to use for sand suspension and for improving water jet performance.

CHAPTER 6: CONCLUSIONS AND RECOMMENDATIONS

Based on the experimental results of this investigation, the following conclusions can be drawn:

1. Design II, presented in this study, allowed efficient injection of slurry upstream of the nozzle in water jetting application, thus providing better momentum transfer to abrasive particles and yielding better results in terms of lower pressure requirement and improved cutting performance.
2. Design II allowed efficient control of abrasive injection rate. Furthermore, abrasive injection rate can be varied easily by controlling engine rpm while water jetting is still in progress without liquid hold-up and air entrainment.
3. Both Xanthan Gum and MF-55 enhanced water jet coherence, which control cutting effectiveness, for a longer distance. However, there is an optimum concentration for both polymers. This optimum concentration was found to be 0.5 % w/w for Xanthan Gum and 0.52% w/w for MF-55.
4. At concentration below 0.5% w/w both Xanthan Gum and MF-55 provide lubrication/drag reduction to flow and thus reduced frictional pressure drop.
5. Xanthan Gum at 1% w/w concentration can suspend sand for more than a week, but MF-55 lacks suspension ability even at concentration of 5% w/w.

This study is but a part of ongoing research effort to improve water jetting performance where it could be useful as an efficient fire extinguishing method to control oil well fire, to clean paraffin deposits inside production tubing, especially at the sand face, and to drill slim laterals down-hole to penetrate well bore skin, which is caused by invasion of reservoir rock by drilling fluids resulting in plugging of rock pores.

In regard to the continuation of this project, the following recommendations are made:

1. Performance of Design II should be evaluated, at higher pressure, to drill oil well casing and pressurized reservoir rock samples to simulate down-hole conditions.
2. Design II should be improved to an extent where the hole drilled is large enough so that the cutting nozzle can follow the drilled hole.
3. Experiments should be conducted to record frictional pressure drop for different lengths of piping between injection point and cutting nozzle. This would be helpful in developing a mathematical model.

REFERENCES

1. William C. Maurer, Joe K. Heilhecker, and William W. Love. (1973). High-Pressure Drilling. SPE. Paper No.3988, pp. 851-859.

2. W. Dickinson and R.W. Dickinson. (1985). Horizontal Radial Drilling System. SPE, Paper No. 13949, pp. 887-892.

3. Wade Dickinson, Herman Dykstra, and Robert Nordlund. (1993). Coiled Tubing Radials Placed by Water Jet Drilling. SPE, Paper No. 26348.

4. N. Brook and D. A. Summers. (1969). The Penetration of Rock by High-Speed Water Jets. Int. J. Rock Mechanics. Sci. Vol 6, pp. 249-258

5. Gene and Vie. Cutting Hard Rock with Abrasive-Entrained Water Jet at Moderate Pressures. Fluidyne Corporation, Auburn, Washington 98002.

6. Summers D.A. and Raether R.J. (1982). Comparative use of Intermediate Pressure Water Jets for Slotting and Removing Concrete. paper J1, Proc 6th Int Symp Jet Cutting Tech, University of Surrey, UK. pp 387-396.

7. Summers D.A. and Peters J.F. (1974). Preliminary Experimentation on Coal Cutting in Pressure Range 35 to 200 MN/m^2. paper H2, Proc 2nd Int. Symp Jet Cutting Tech, Cambridge UK.

8. N.J. Griffiths and M.A. Cantab. Abrasive Injection Usage in The United Kingdom. Sheldon Industrial Equipment, Burmingham, England.

9. Mohamed Hashish. Experimental Studies of Cutting with Abrasive Water Jets. Flow Industries, Inc., Washington.

10. Baumann L. and Henneke J. (1980). Attempt of Technical-Economical Optimization of High Pressure Jet Assistance for Tunneling Machines. Paper c4, 5th Int Symp Jet Cutting Tech, Hanover Germany. pp 119-140.

11. Barton, R.E.P., and Saunders, D.A., (1982). Water/Abrasive Jet Cutting of Concrete and Reinforced Concrete. Proceedings of The Sixth International Symposium on Jet Cutting Technology, BHRA Fluid Engineering, Cranfield, England. pp. 489-502.

12. Hashish, M. 1982b. Steel Cutting with Abrasive Water Jet. Proceedings of the Sixth International Symposium on Jet Cutting Technology, BHRA Fluid Engineering, Cranfield England, pp. 465-487.

13. R.K. Swanson, M. Kilman, S. Cerwin, and W. Tarver. Study of Particle Velocities in Water Driven Abrasive Jet Cutting. Southwest Research Institute, San Antonio, Texas.

14. Hashish, M., (1984). A Modeling Study of Metal Cutting with Abrasive Water Jet. Trans. ASME, Vol. 106, pp. 88-100.

15. http://www. bhrgroup.co.uk/daijet/technology.html. Retrieved on 06/16/2005

16. S.V. Chacko, A. Gupta, D.A. Summers. (2003). Comparative Performance Study of Polyacrylamide and Xanthan Polymer in Abrasive Slurry Jet. University of Missouri-Rolla, U.S.A.

17. Graettinger, Johnson, Sewell and Wagner. (2002) Foundation Evaluation with Micro Intrusive Testing. The University of Tuscaloosa, Tuscaloosa, Alabama. UTCA Report #01114.

18. Hoyt, J.W. (1972) Turbulent Flow of Drag-Reducing Suspension. U.S. Naval Undersea R &D Center Report, NUCTP 299.

19. Savins, J.G. Drag Reduction Characteristics of Solutions of Macromolecules in Turbulent Pipe Flow. Petrol. Engr. 4,3 pp.-203-13.

20. New Scientist (Number 380), Feb 1964.

21. Summers, D.A. (May 1968). Ph.d. Thesis, University of Leeds, Department of Applied Mineral Sciences.

22. W.G. Howells. Polymerblasting – A Chemist’s Point of View, Berkely Chemical Research, Inc. Berkely, California.

23. White, A. and Hemmings, J.A.G.(1976). Drag Reduction by Additives. Review and Bibliography, BHRA Fluid Engineering, 1976.

24. Momber and Kovacevic. (1998). Principle of Abrasive Water Jet Machining. Great Britain. Springer.

25. http://www.scientificpsychic.com/fitness/carbohydrates. Retrieved on 06/20/2005.

APPENDIX: EXPERIMENTAL DATA AND JET FIGURES

Table A-1 Experimental Data of Pump Performance Curves

Pressure (Psig) **Flow Rate (GPM)**	**Open Flow**	**500 Psig**	**1000 Psig**	**1500 Psig**	**2000 Psig**	**2500 Psig**
2.5	X	1834	1869	2000	X	X
2.7	X	2086	2129	X	2211	X
2.8	X	X	X	2198	X	X
2.9	X	X	X	X	2399	X
3	X	X	2330	2355	X	2521
3.1	2250	X	X	X	X	X
3.2	X	2343	2497	2570	2565	2670
3.4	X	X	X	X	2777	X
3.5	X	X	2661	X	X	2871
3.6	X	2726	X	X	X	X
3.7	2680	X	2885	2957	X	X
3.8	X	X	X	X	3008	3127
4.0	X	X	X	X	X	3259
4.1	3010	3084	3086	3150	3235	X
4.2	X	X	X	X	3390	3431
4.3	3200	3237	3308	3375	X	X

Table A-2 Calculated and Measured Flow Rate

Pressure (Psig)	RPM	Calculated Flow Rate (GPM)	Measured Flow Rate (GPM)
OPEN	**2250**	3.06	3.1
	2680	3.64	3.7
	3010	4.09	4.1
	3200	4.35	4.3
500	**1834**	2.44	2.5
	2086	2.77	2.7
	2343	3.12	3.2
	2726	3.63	3.6
	3084	4.1	4.1
	3237	4.31	4.3
1000	**1869**	2.43	2.5
	2129	2.77	2.7
	2330	3.03	3
	2497	3.25	3.2
	2661	3.46	3.5
	2885	3.75	3.7
	3086	4.01	4.1
	3307	4.3	4.3

Table A-2 Continued

Pressure (Psig)	RPM)	Calculated Flow Rate (GPM)	Measured Flow Rate (GPM)
1500	**2000**	2.54	2.5
	2198	2.79	2.8
	2355	2.99	3
	2570	3.26	3.2
	2745	3.49	3.5
	2957	3.76	3.7
	3149	4	4.1
	3375	4.29	4.3
2000	**2211**	2.74	2.7
	2399	2.97	2.9
	2565	3.18	3.2
	2777	3.44	3.4
	3009	3.73	3.8
	3235	4.01	4.1
	3390	4.2	4.2
2500	**2521**	3.05	3
	2671	3.23	3.1
	2871	3.47	3.5
	3259	3.94	4
	3431	4.15	4.2

Table A-3 Jet Lengths as Obtained from GIMP®

Total Flow Rate GPM	Loading Ratio	Polymer Concentration % w/w	Xanthan	Mf-55	Only Water
4.4	0.7	0.40	1.52	1.60	1.2
4.5	0.8	0.44	1.87	1.95	1.1
4.8	0.9	0.47	2.25	2.67	1
5	1	0.50	2.44	3.43	0.95
5.3	1.1	0.52	2.12	3.65	0.9
5.5	1.2	0.55	2.05	2.60	0.85
5.8	1.3	0.57	1.43	2.03	0.79
5.9	1.4	0.59	1.32	1.77	0.72

Table A-4 Experimental Pressure Data for Polymers and Water to Flow through 0.069 inches Diameter Nozzle

Injection Rate from Accumulators (GPM)	Pressure	Xanthan (PSIG)	MF-55 (PSIG)	Only Water (PSIG)
	Total Flow through 0.069" Nozzle			
1.75	4.4	1070	1070	1090
2	4.5	1200	1200	1220
2.25	4.8	1330	1300	1350
2.5	5	1500	1480	1500
2.75	5.3	1630	1610	1630
3.0	5.5	1800	1780	1800
3.25	5.8	2000	1950	2000
3.5	5.9	2150	2110	2150

Table A-5 Experimental Pressure Drop Data across the Accumulator for Xanthan

Xanthan Injection Rate (GPM)	P_2 (PSIG)	P_1 (PSIG)	ΔP
1.8	1170	1070	100
2	1310	1200	110
2.3	1460	1330	130
2.5	1650	1500	150
2.8	1780	1630	150
3.0	1970	1800	170
3.3	2180	200	180
3.5	2350	2150	200

TABLE A-6 Experimental Pressure Drop Data across the Accumulator for MF-55

MF-55 Injection Rate (GPM)	P_2 (PSIG)	P_1 (PSIG)	ΔP
1.8	1150	1070	80
2	1290	1200	90
2.3	1410	1300	110
2.5	1610	1480	130
2.8	1740	1610	130
3.0	1920	1780	140
3.3	2110	1950	160
3.5	2280	2110	170

Table A-7 Experimental Pressure Data across the Accumulator for Water

Water Injection Rate (GPM)	P_2 (PSIG)	P_1 (PSIG)	ΔP
1.8	1150	1090	60
2	1290	1220	70
2.3	1430	1350	80
2.5	1590	1500	90
2.8	1700	1600	100
3.0	1880	1770	110
3.3	2060	1930	130
3.5	2190	2050	140

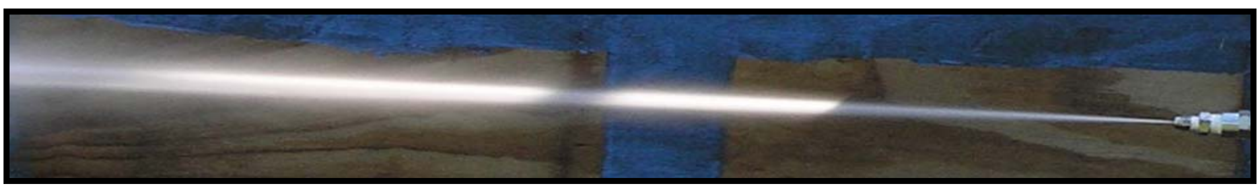

(a)

(b)

(c)

Figure A-1 Jet Images of, (a) Water (4.4 gallons per minute), (b) Xanthan (0.40% w/w, Injection Rate of 1.8 gallons per minute), and, (c) MF-55 (0.40% w/w, Injection Rate of 1.8 gallons per minute)

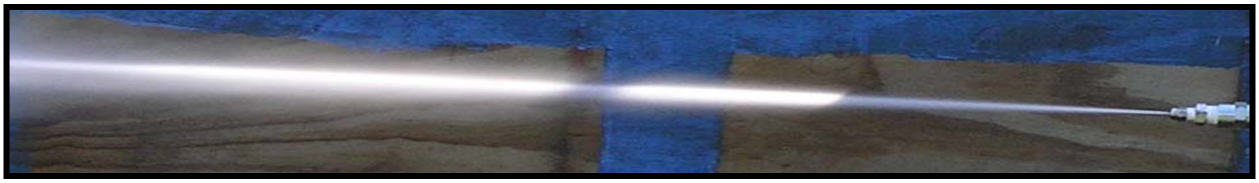

(a)

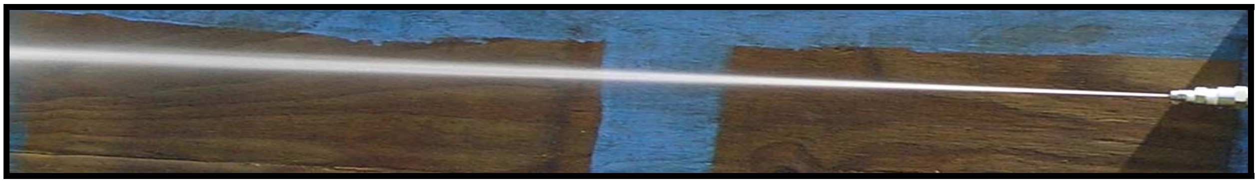

(b)

(c)

Figure A-2 Jet Images of, (a) Water (4.5 gallons per minute), (b) Xanthan (0.44% w/w, Injection Rate of 2.0 gallons per minute), and, (c) MF-55 (0.44% w/w, Injection Rate of 2.0 gallons per minute)

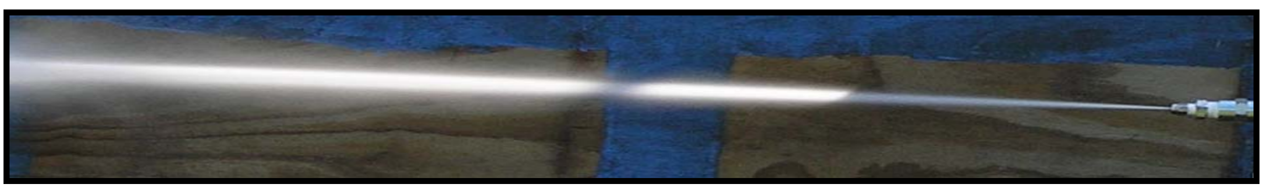

(a)

(b)

(c)

Figure A-3 Jet Images of, (a) Water (4.8 gallons per minute), (b) Xanthan (0.47% w/w, Injection Rate of 2.3 gallons per minute), and, (c) MF-55 (0.47% w/w, Injection Rate of 2.3 gallons per minute)

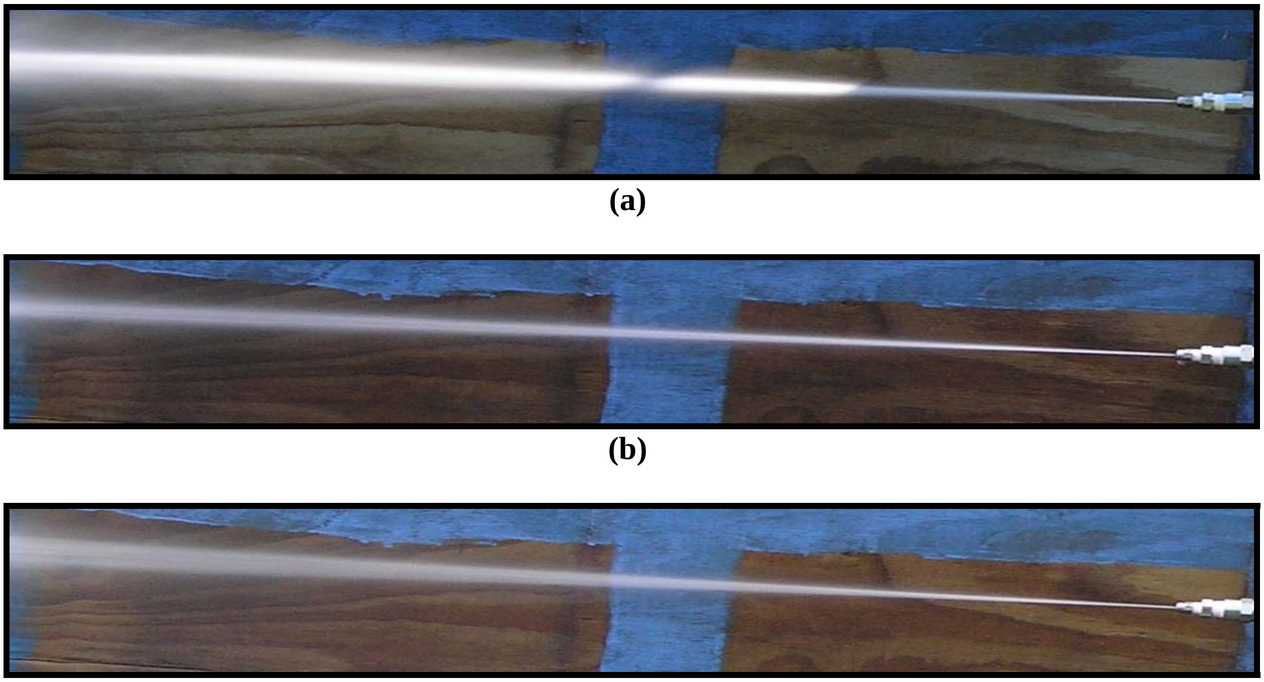

(a)

(b)

(c)

Figure A-4 Jet Images of, (a) Water (5.0 gallons per minute), (b) Xanthan (0.50% w/w, Injection Rate of 2.5 gallons per minute), and, (c) MF-55 (0.50% w/w, Injection Rate of 2.5 gallons per minute)

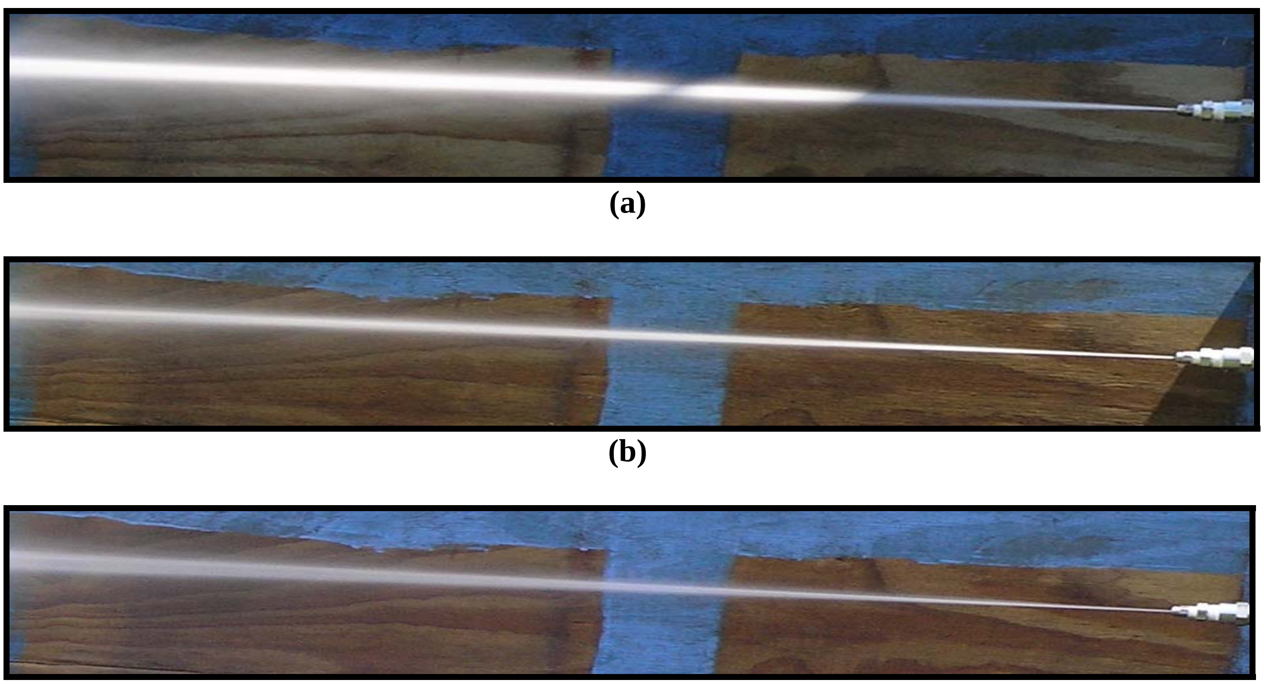

(a)

(b)

(c)

Figure A-5 Jet Images of, (a) Water (5.3 gallons per minute), (b) Xanthan (0.52% w/w, Injection Rate of 2.8 gallons per minute), and, (c) MF-55 (0.52% w/w, Injection Rate of 2.8 gallons per minute)

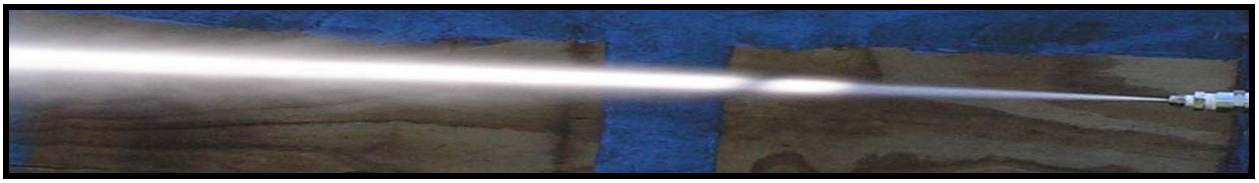

(a)

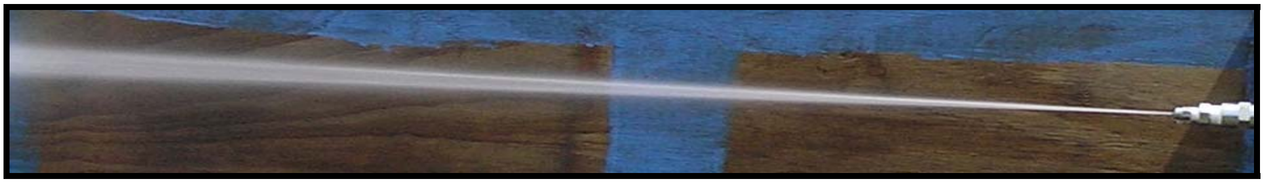

(b)

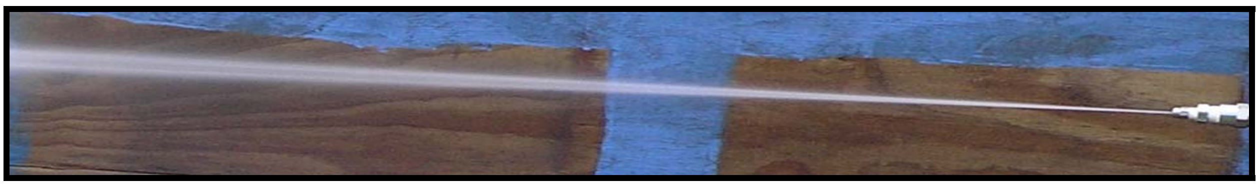

(c)

Figure A-6 Jet Images of, (a) Water (5.5 gallons per minute), (b) Xanthan (0.55% w/w, Injection Rate of 3.0 gallons per minute), and, (c) MF-55 (0.55% w/w, Injection Rate of 3.0 gallons per minute)

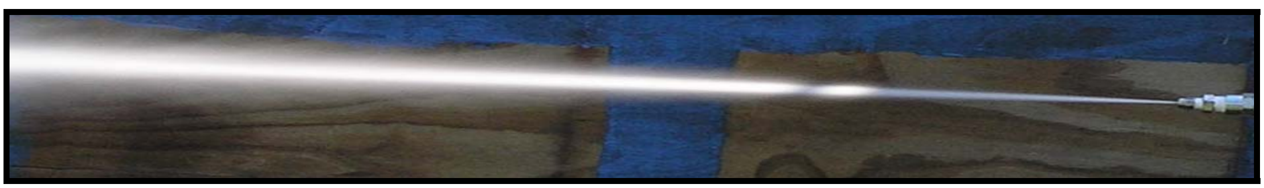

(a)

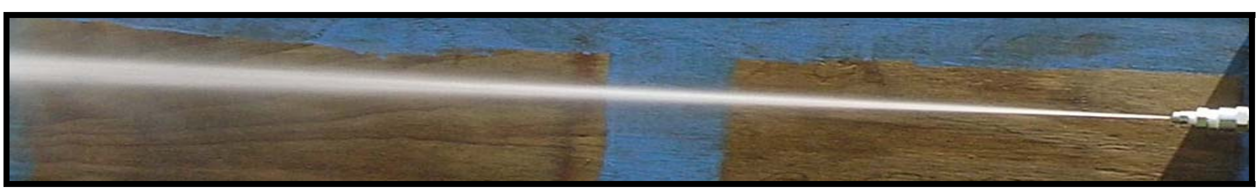

(b)

(c)

Figure A-7 Jet Images of, (a) Water (5.8 gallons per minute), (b) Xanthan (0.57% w/w, Injection Rate of 3.3 gallons per minute), and, (c) MF-55 (0.57% w/w, Injection Rate of 3.3 gallons per minute)

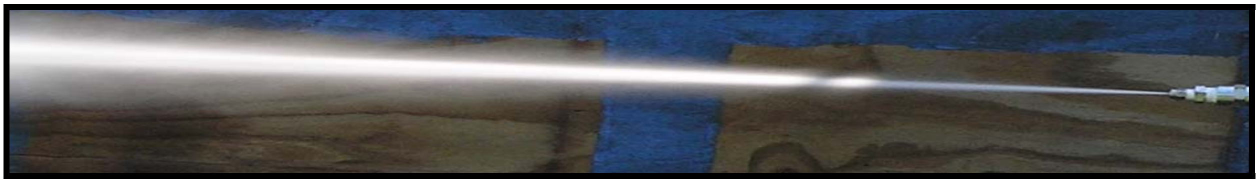

(a)

(b)

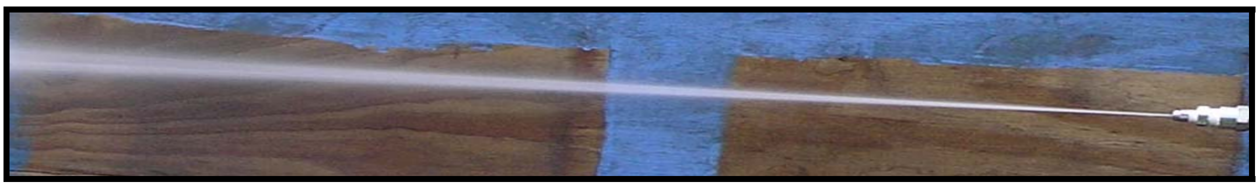

(c)

Figure A-8 Jet Images of, (a) Water (6.0 gallons per minute), (b) Xanthan (0.59% w/w, Injection Rate of 3.5 gallons per minute), and, (c) MF-55 (0.59% w/w, Injection Rate of 3.5 gallons per minute)

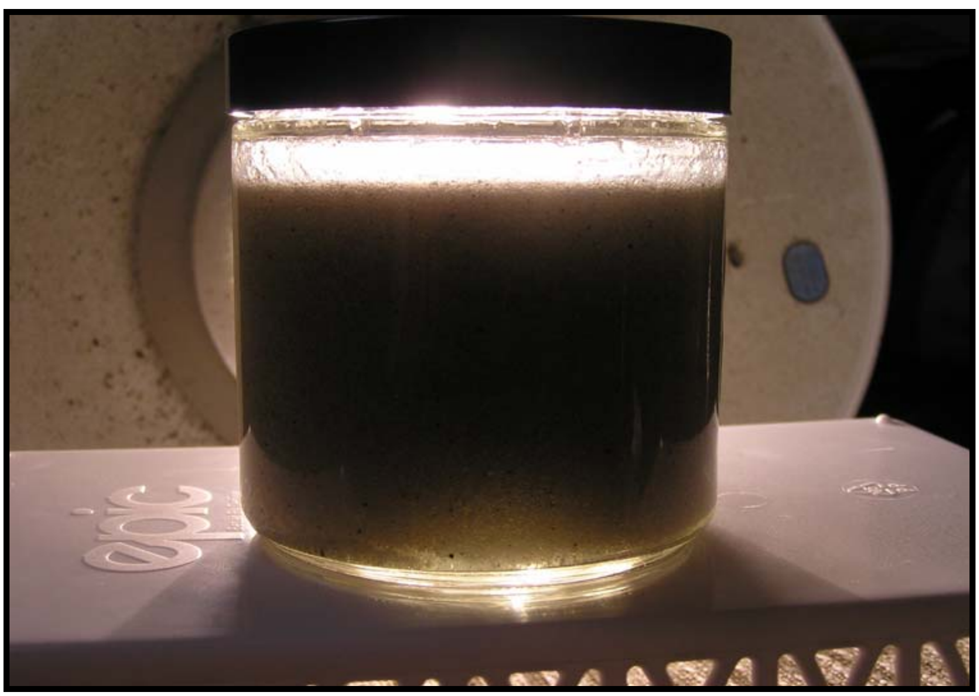

Figure A-9 Xanthan 1% (w/w) Sand (150 gms) Suspension Test, After One Week

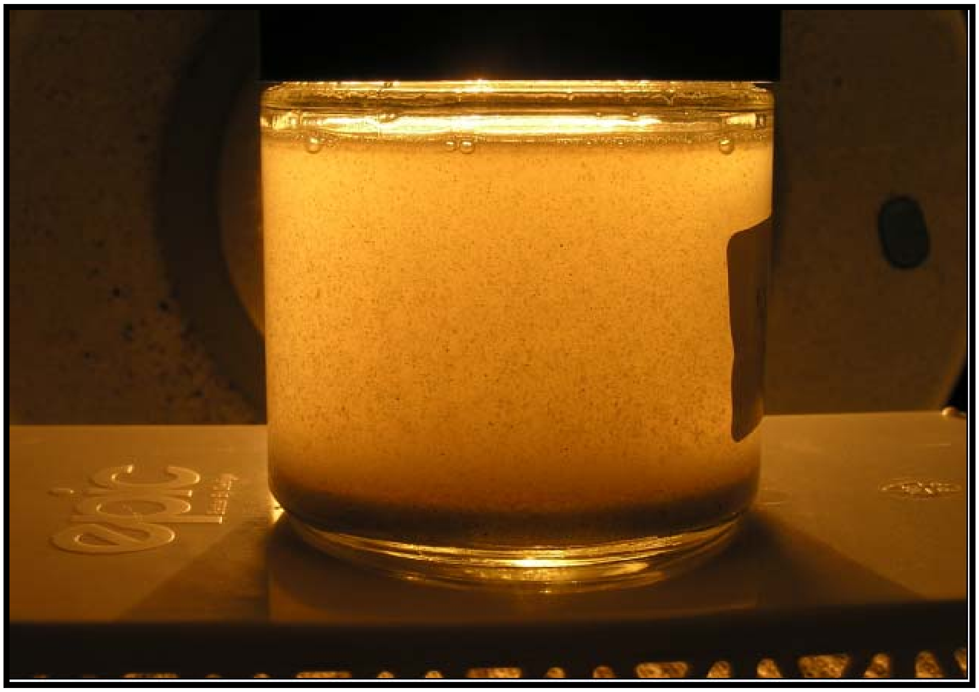

(a)

(b)

Figure A-9 Xanthan 0.25% w/w Sand Suspension Test, (a) After 20 seconds, (b) After 60 seconds

(a)

(b)

Figure A-10 Xanthan 0.38% w/w Sand Suspension Test, (a) After 20 seconds, (b) After 60 seconds

(a)

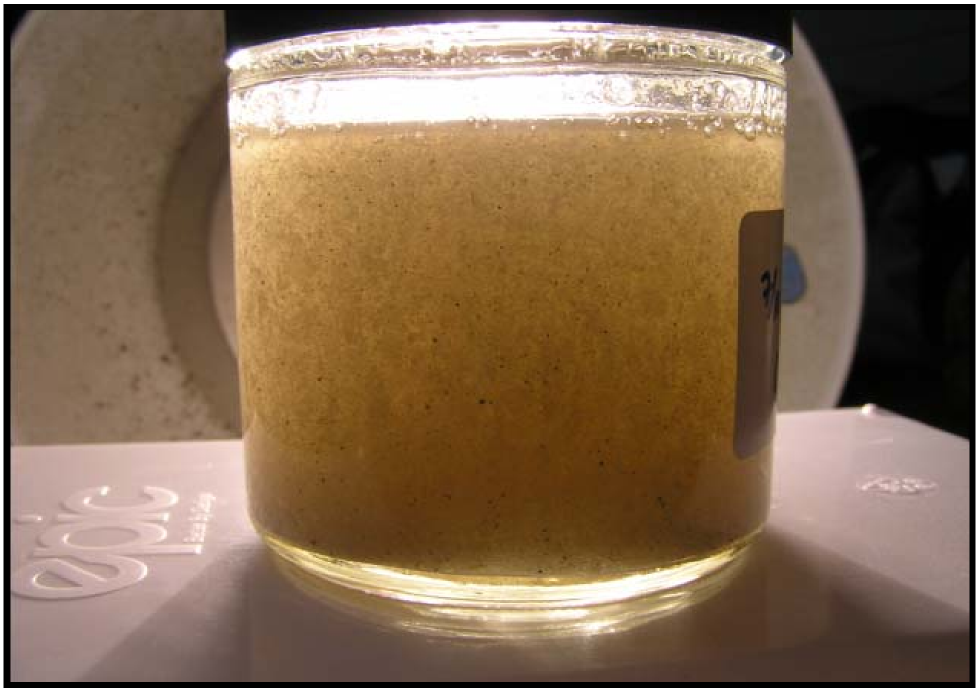

(b)

Figure A-11 Xanthan 0.44% w/w Sand Suspension Test, (a) After 60 seconds, (b) After 30 minutes

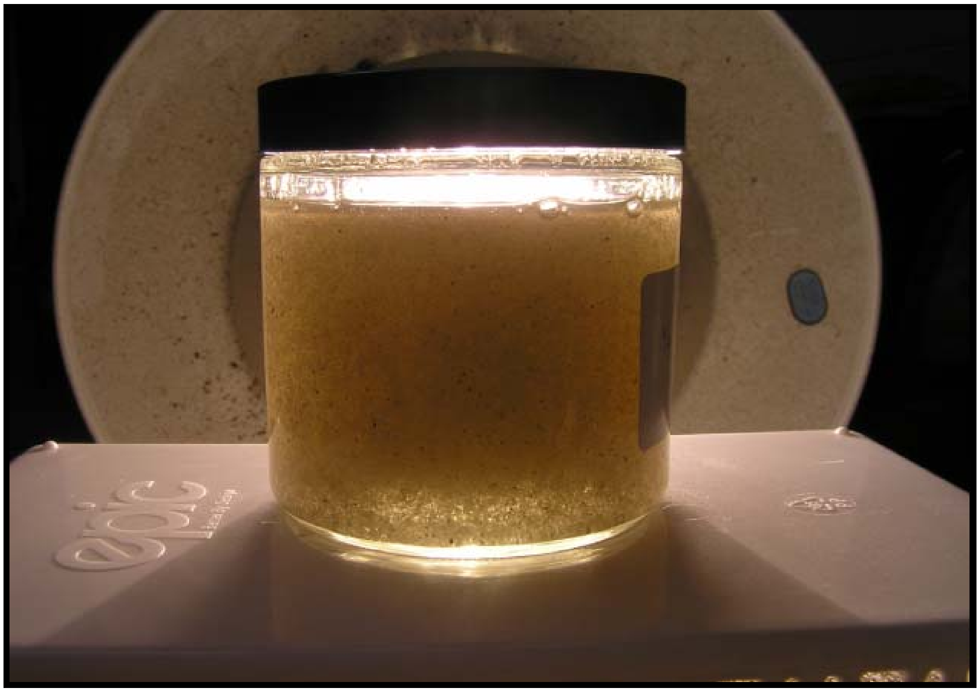

(a)

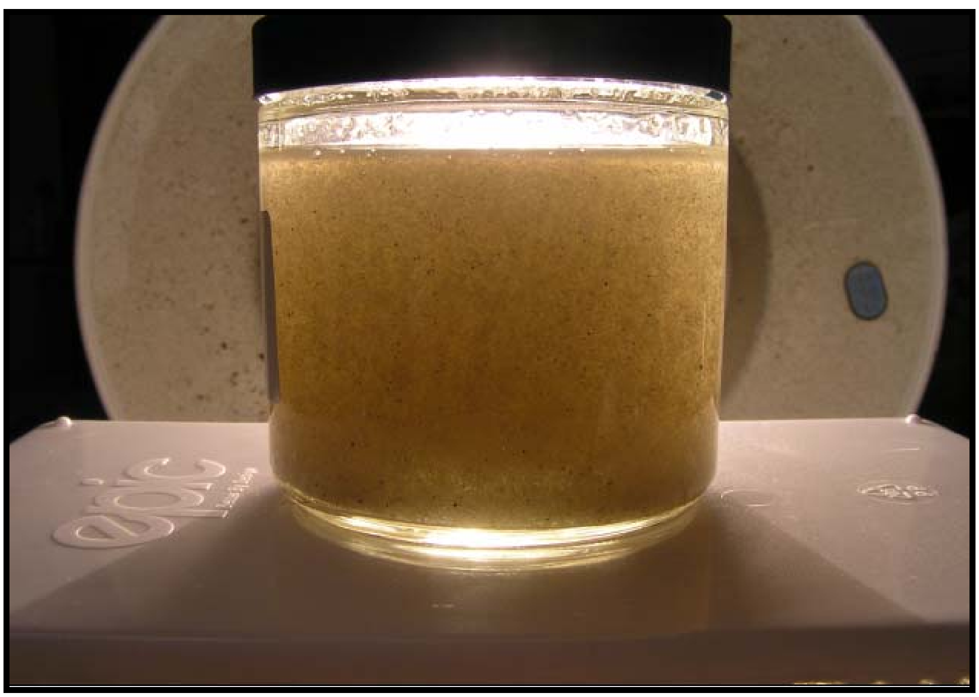

(b)

Figure A-12 Xanthan 0.50% w/w Sand Suspension Test, (a) After one hour, (b) After three hours

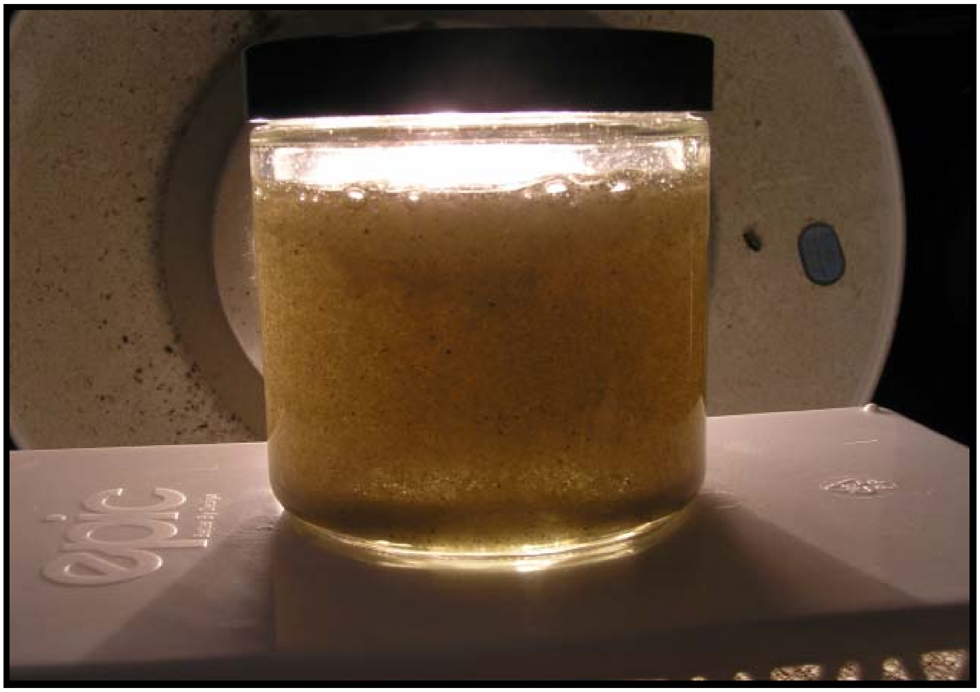

(a)

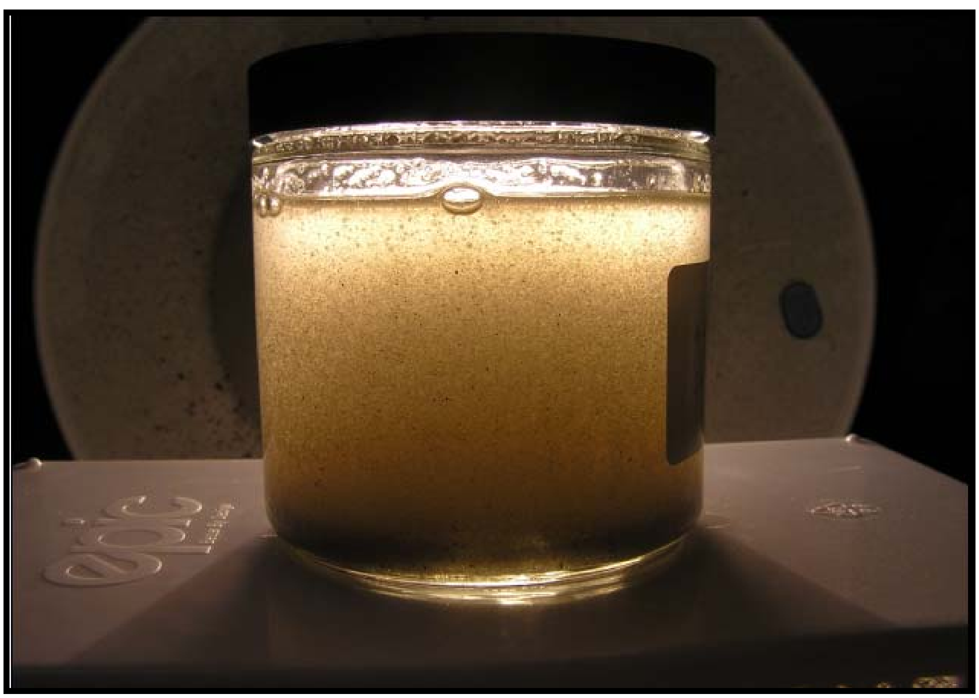

(b)

Figure A-13 CMC 6.5% w/w Sand Suspension Test, (a) After 20 seconds, (b) After 30 minutes

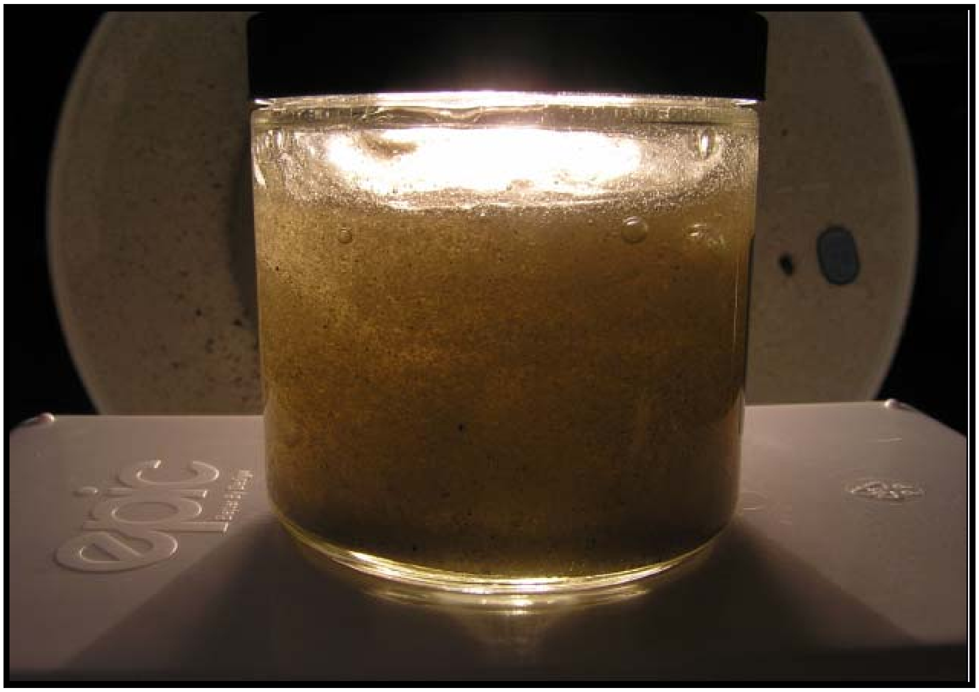

(a)

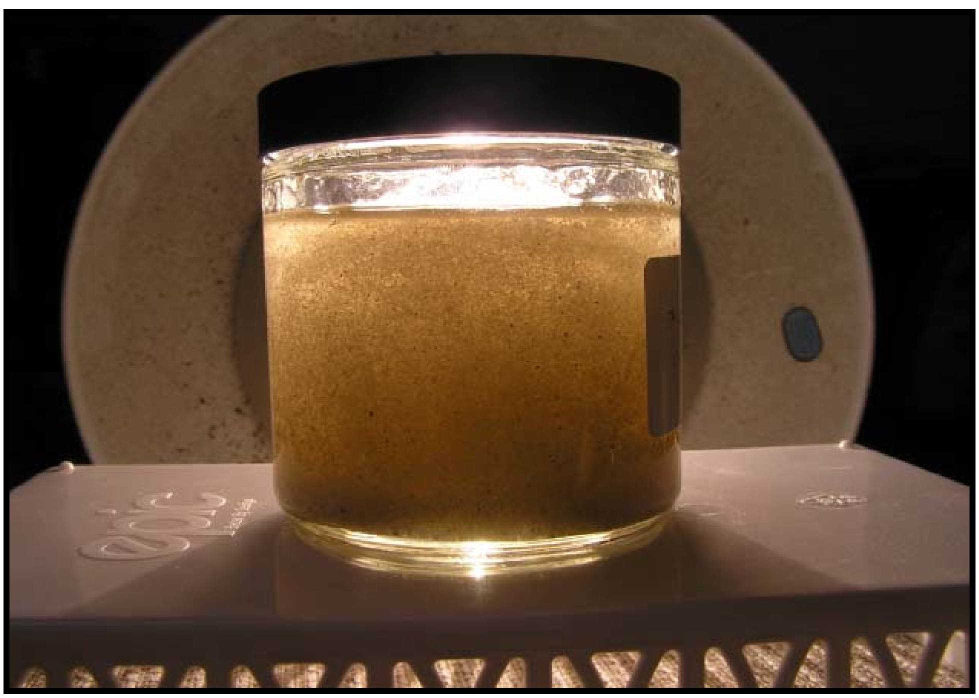

(b)

Figure A-14 CMC 7.5% w/w Sand Suspension Test, (a) After 20 seconds, (b) After 30 minutes

VITA

Manish Kumar was born on September 21, 1981, in Sidhrawali, a village in Haryana, India. He attended Rao Lal Singh Public School till eighth grade, and then transferred to Dayanand Anglo Vedic Public School, Gurgaon, Haryana, from where he graduated in May of 1998. Manish attended Maharshi Dayanand University, Rohtak, India, and received a Bachelor of Engineering Degree in Chemical Engineering in May of 2002. He joined the Graduate School at University of Missouri-Rolla in January of 2003, and transferred to Louisiana State University in January of 2004, to continue his research work and, to obtain the degree of Master of Science in Petroleum Engineering.